PARAMETRIC STUDY AND FEEDBACK CONTROL OF METHANOL STEAM REFORMING REACTION IN A MICRO-CHANNEL REACTOR

A Thesis

by

KUNAL DAS

Submitted to the Office of Graduate and Professional Studies of
Texas A&M University
in partial fulfillment of the requirements for the degree of

MASTER OF SCIENCE

Chair of Committee,	Benjamin Wilhite
Committee Members,	Costas Kravaris
	Andrea Strzelec
Head of Department,	M. Nazmul Karim

May 2017

Major Subject: Chemical Engineering

ABSTRACT

A 1-dimensional dynamic state simulation model has been developed to study methanol steam reforming reaction in a micro-channel reactor heated using a heating plate. Conversion and temperature profiles along the length of the micro-channel and with respect to time have been investigated. Firstly, the effect of material of construction of the micro-channel reactor on the open loop dynamic responses for conversion and temperature were investigated. Secondly, state space models for conversion were derived for 3 different materials of construction (Stainless steel 316, Silicon and Aluminum). A proportional integral (PI) controller using a Hammerstein model is used to study the closed loop dynamic response for the state space model. Also, the effect of varying the controller parameters on the response times of the system has been investigated. Finally, the partial differential equations (PDE) model is used to run the closed loop simulations using a PI controller with Hammerstein model and the results of the state space model and the PDE model are compared. All simulations were carried out using MATLAB R2016a®. The results obtained showed that settling time of around 10 seconds to 30 seconds can be achieved in the micro-reactors when using a PI controller in closed loop. Silicon showed the best settling times out of the three materials considered in this research.

ACKNOWLEDGEMENTS

I would like to express the deepest appreciation to my committee chair Dr. Benjamin A. Wilhite and committee co-chair Dr. Costas Kravaris, who have continually and convincingly conveyed a spirit of adventure about research. Without their guidance and persistent help this dissertation would not have been possible.

I would like to thank my committee member, Dr. Andrea Strezlec, who has gone out of her way to help when I needed it. Her work was an inspiration for this research.

In addition, I would like to thank the Artie McFerrin Department of Chemical Engineering for providing every support, ranging from scholarships to laboratory, for making this possible. Without the constant help from the faculty members, the department head and the brilliant administrative workforce of this department, this research would not be possible.

Lastly, I would like to thank my parents, for always supporting me and for assuring me that I would be successful. Words won't do justice to how indebted I am to them for always being there and letting me follow my dreams and supporting me no matter what.

CONTRIBUTORS AND FUNDING SOURCES

This work was supervised by a thesis committee consisting of Professor Benjamin Wilhite and Professor Costas Kravaris of the Department of Chemical Engineering and Professor Andrea Strezlec of Department of Mechanical Engineering.

All work for the thesis was completed independently by the student.

There are no outside funding contributions to acknowledge related to the research and compilation of this document.

TABLE OF CONTENTS

LIST OF FIGURES

LIST OF TABLES

CHAPTER I

INTRODUCTION

Fuel cell technology is amongst the most promising technologies for the conversion of chemical energy into electrical energy (Dyer, 2002). Fuel cells are considered as clean energy sources with widespread application where it can replace conventional batteries and can be used in laptop, mobile phones, car engine and even as an alternative for gasoline or diesel engines (Breen, 2002). The major impediment for the fuel cell technology is the storage of pure hydrogen which is the fuel for fuel cells (Chalk, 2006). To this end, reforming reactions which can produce hydrogen in-situ with the fuel cells are of interest (Palo, 2007). There exist numerous reforming techniques to produce hydrogen including auto-thermal reforming, steam reforming and partial reforming (Brown, 2001).

Micro reactors have several fundamental advantages as the miniaturization helps in portability, better control of fast reactions, shorter response times amongst others (Ehrfeld, 2002). The characteristic dimensions of one channel in a micro reactor ranges from sub-micrometer to the sub-millimeter regime. The material of construction of a micro reactor is typically a metal. Micro reactors are generally classified into three categories – Singular type, Capillary type and Micro structured (Serra, 2013). Fig. 1 shows a market available glass micro reactor (Amar Equipments, 2016).

Micro reactors are better than conventional reactors in case of highly endothermic reactions as they require a higher surface area to volume ratio. Methanol steam reforming reaction is a lucrative option for producing hydrogen for use in fuel cells. The reaction is presented as (Peppley, 1999)–

$$CH_3OH + H_2O \rightarrow CO_2 + 3H_2 \qquad \Delta H_f = 49.4 \text{ KJ/mol}$$

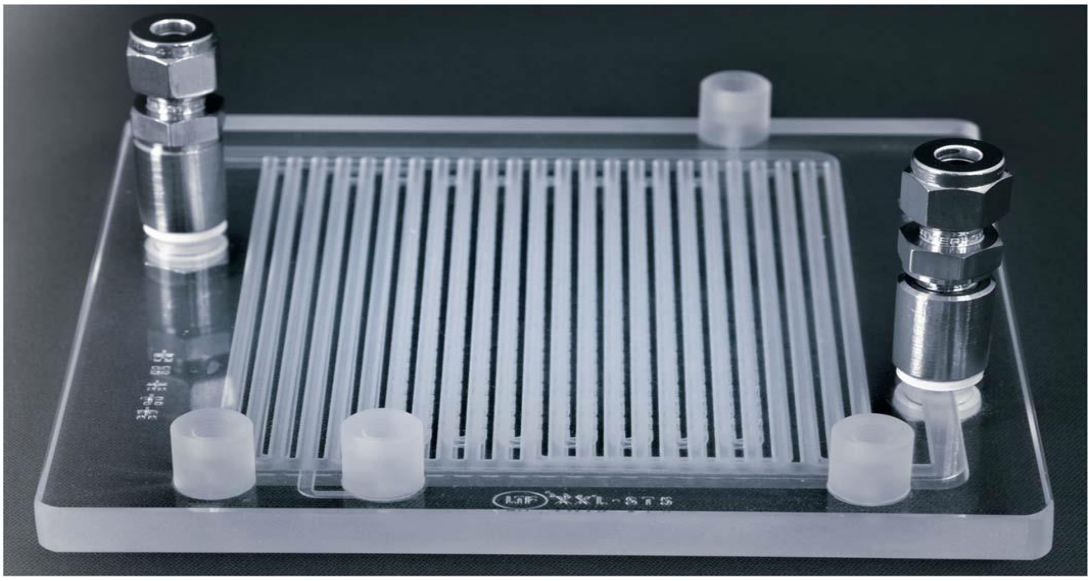

Fig. 1 –Reprinted from Amar Equip, 2016, Photo of a commercial glass micro reactor

Methanol molecule has a 4:1 hydrogen-carbon ratio and hence can be considered as a chemical storage for hydrogen. Methanol, due it liquid state at ambient temperature, is much easier to transport when compared to pure hydrogen (Vazquez, 2015). Also, the absence of C-C bonds unlike in the higher hydrocarbons, makes the steam reforming possible at lower temperature (Olah, 2006). Methanol steam reforming (MSR) is a highly endothermic reaction which is thermodynamically favorable at temperature ranges of 200˚C to 400˚C (Peppley, 1999). The highly endothermic nature of the methanol steam reforming reaction makes the need for heat transfer throughout the reactor very important and this leads to the sub-par performance of the conventional reactors like packed bed reactors, fixed bed reactors etc. for the reforming reaction (Echave, 2013). Micro-channel reactors offer an optimal solution for the steam reforming of methanol due to their improved heat and mass transfer properties. Micro-reactors also provide scope for better control of temperature inside the micro-reactor and lead to reduction of hot spots. (Kolb, 2005). Micro-channels are normally wall coated with catalysts and hence most of the reactions occurs at the wall which leads to a higher surface area to volume ratio for a micro-channel reactor (Pan, 2015).

The thermal properties of the material of build of the micro-channel reactor is of great importance for MSR because of its highly endothermic nature. Heat provided for the reaction passes on to the reacting fluid through the reactor wall (Kundu, 2006). Different types of heaters are available to heat a block of micro-reactor ranging from Rigid heating mantles, block heaters to circulation jackets. Control of MSR inside a micro-reactor is a challenging hurdle to be overtaken for successful implementation of this technology in fuel cells for cars. Due to the variable power requirements of a car engine at different times, the hydrogen production in the micro-reactor system must be controlled. PID controllers are mostly used in process control for micro-reactors (Dinca, 2008). For easier system control and non-linear systems, state space models are often estimated for complex models (Verhaegen, 1994).

Different types of catalysts are present in the literature for MSR. Copper based catalysts are most abundantly used due to their high activity and selectivity (Takahashi, 1982). Copper based oxides are known to be deactivated by thermal sintering and hence other catalyst are being actively studied (Karim, 2008). Pd/ZnO catalysts provides better resistance to thermal sintering but produces less hydrogen when compared to hydrogen based catalysts (Suwa, 2004).

Control strategies for conventional reactor have been studied extensively in literature (Kendall, 2006). A parametric study helps in the scale up of the process for industrial application (Moreno, 2008). The temperature profile inside a micro-reactor is of significant concern so as not to produce any hot zones (TeGrotenhuis, 2008). Controlling the reaction rate to produce variable amounts of hydrogen at different times is of considerate interest (Tronconi, 2005).

For this study, different materials have been considered based on their thermal properties for building the micro-reactor. Specifically, SS316, Aluminum and Silicon were selected, based on

their diverse thermal properties, to carry the simulations out on. Conversion and temperature profiles were developed along the length of a micro-channel and with respect to time. The kinetics for the reaction were considered as for reaction occurring on a Pd/ZnO wall coated catalyst (Cao, 2003). Step responses were studied and a state space model was developed to carry out closed loop simulations. The veracity of the closed loop responses of the state space model was compared to the control responses of the actual model.

A state space model helps in studying control of nonlinear systems and with systems with multiple input and multiple outputs (Smith, Estimating a State-Space Model from Point Process Observations, 2003). The control limitations of a PI controller for a nonlinear first order process have been studied in-depth in literature (Anandanatarajan, 2005).

Fig. 2 shows a plausible model of a micro reactor block coupled with a fuel cell which can be used in an automobile engine. Methanol and steam is passed to the micro-reactor for reforming reaction which produces carbon dioxide and hydrogen along with unreacted methanol and steam. The separator separates the hydrogen and sends it to the fuel cell and the other components are sent for combustion. The combustion of the unreacted methanol produces heat which coupled with the micro-reactor, can provide the heat required for the steam reforming reaction.

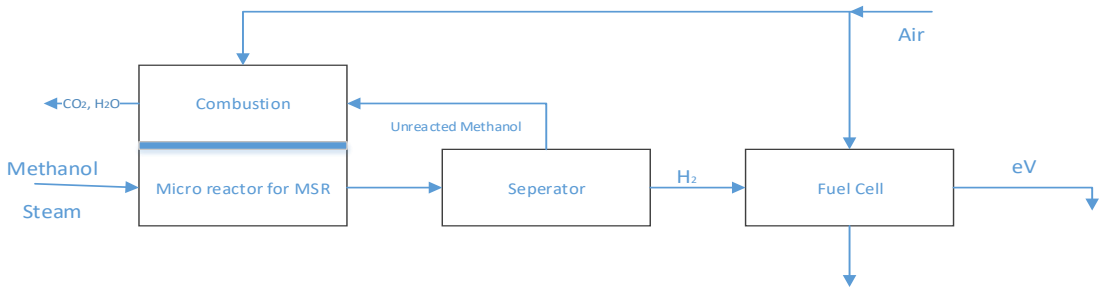

Fig. 2 – Micro reactor coupled with fuel cell for automobile use

CHAPTER II

METHODOLOGY

2.1) Introduction

The methanol steam reforming (MSR) reaction in a micro-channel reactors a lucrative option for portable hydrogen production. To make MSR in a micro-channel reactor a viable option for implementation in dynamic processes like for example, a car engine, the unsteady state control assumes interest. Fig. 3 (Kundu, 2006) presents a photo of a micro-channel reactor. For the model formulation, one channel of a micro-reactor was considered.

Fig. 3 – Reprinted from Kundu, 2006, Photo of a micro-reactor unit

In the coming section, a generic unsteady state mass and energy balance model for an endothermic reaction in a micro-channel reactor with a heating plate was derived. The generic model can be implemented for any endothermic reaction in a micro-reactor by using appropriate values for reaction rate and building material of the micro-reactor.

2.2) Model formulation

In this study, a 1-D model of a MSR reaction in a micro-channel reactor (Echave, 2013) was formulated. A schematic of a single micro-channel reactor is shown in Fig. 4. A generic endothermic reaction, where reactant 'A' converts to product 'B,' is used for deriving the mass balance and energy balance equations.

A → B (endothermic) …… (I)

The rate expression for reaction (I) is given by an Arrhenius temperature dependent power law kinetics

(2.1) …… $r_j = -k_o \exp\left[\frac{-E_a}{RT}\right] C_A^n$

2.2.1) Derivation for unsteady state mass expression

Considering plug flow in a reactor for component j, with inlet flowrate, F_{jo}, and outlet flowrate, F_j, for a small volume dv at an unsteady state with the rate expression given by eq. (2.1) and where N_j is the number of moles of reactant; mass balance can be represented by (Levenspiel, 1962) -

(2.2) …… $F_{jo} - F_j + \int_0^{dv} r_j \, dv = \frac{dN_j}{dt}$

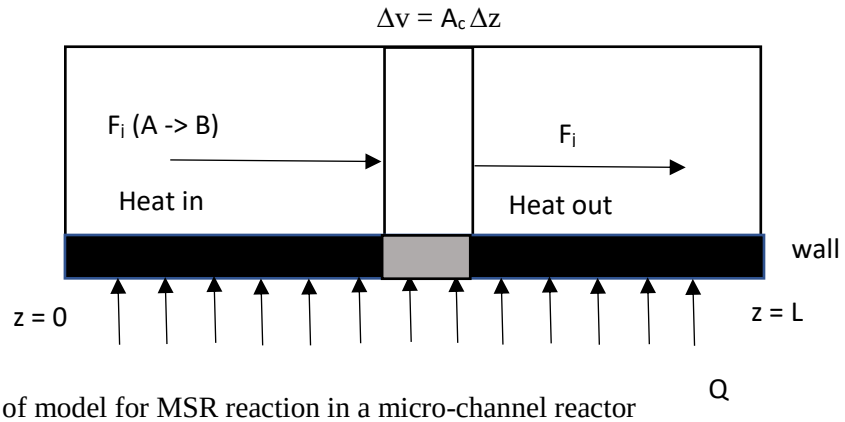

Fig. 4 – Schematic of model for MSR reaction in a micro-channel reactor

Assuming uniform differential plug flow,

$\int_0^{dv} r_j \, dv = r_j \, v$

At unsteady state, assuming steady-state velocity, there is no accumulation with respect to time, hence

$\Delta v \ \frac{dN_j}{dt} = F_{j,in} - F_{j,out}$

$\frac{dN_j}{dt} = \Delta v \frac{dC_j}{dt}$ (C is the concentration)

When a small volume section, Δv, is considered, eq. (2.2) can be written as

(2.3) …… $F_j(z) - F_j(z+\Delta z) + r_j \, \Delta v = \Delta v \frac{dC_j}{dt}$

For a uniform cross sectional area (A) and length (L), eq. (2.3) transforms to

$F_j(z) - F_j(z+\Delta z) + r_j \, A\Delta z = A\Delta y \frac{dC_j}{dt}$

(2.4) …… $[F_j(z) - F_j(z+\Delta z)] / A\Delta z + r_j = \frac{dC_j}{dt}$

In differential form, eq. (2.4) simplifies to

$-\frac{1}{A}\frac{dFj}{dy} + r_j = \frac{dC_j}{dt}$

$\frac{dC_j}{dt} = -v_o \frac{dC_j}{dy} - k_j \exp\left[\frac{-E_{aj}}{RT}\right] C_j^n$

Where v_o is the velocity of the flow of reacting fluid. The generalized form of the mass balance equation for reaction (I) can be represented as

$$(2.5) \ldots\ldots\ldots \quad \frac{dC_A}{dt} = -v_o \frac{dC_A}{dz} - k_o \exp\left[\frac{-E_a}{RT}\right] C_A^n$$

Boundary condition and initial condition –

As the PDE is first order in time and spatial dimension, one boundary condition and one initial condition were defined. Boundary condition of zero conversion for methanol at the inlet of the micro-channel was considered.

(B.C. 1) …… $C_A = C_{A,f}$ at $z = 0$

Initially, no conversion was assumed for all points of the micro-channel.

(I.C. 1) …… $C_A = C_{A,f}$ at $t = 0$

2.2.2) Derivation for unsteady state energy expression

The unsteady state energy balance in an ideal plug flow reactor is given by (Froment, 1990) -

(2.6) …… Accumulation = Heat in – Heat Out + Heat Generated

For a differential volume, Δv, with the density considered to be a constant, ρ, the specific heat, C_p ,

(2.7) …… Accumulation in an unsteady state = $\Delta v \rho C_p \frac{dT}{dt}$

(2.8) …… Heat in can be represented as = $F_AH_A + F_BH_B$

Where F_A is the inlet flowrate of the reactant A, H_A is the inlet enthalpy of the reactant A, F_B is the inlet flowrate of the product B and H_B is the inlet enthalpy of the product B.

(2.9) …… Heat out can be represented as = $(F_A+dF_A)(H_A+ dH_A) + (F_B+dF_B)(H_B+ dH_B)$

Where (F_A+dF_A) is the outlet flowrate of the reactant A, $(H_A+ dH_A)$ is the outlet enthalpy of the reactant A, (F_B+dF_B) is the outlet flowrate of the product B and $(H_B+ dH_B)$ is the outlet enthalpy of the product B.

Combining eqns. (2.7), (2.8) and (2.9) and considering dQ to be the heat generated in the dV volume, eq. (2.6) can be written as

$$\Delta v\rho C_p\frac{dT}{dt} = F_AH_A + F_BH_B - (F_A+dF_A)(H_A+ dH_A) - (F_B+dF_B)(H_B+ dH_B) + dQ$$

Now dividing by dV and simplifying , gives

$$\frac{dQ}{dV} = F_A\frac{dH_A}{dV} + F_B\frac{dH_B}{dV} + dF_A\frac{dH_A}{dV} + dF_B\frac{dH_B}{dV} + H_A\frac{dF_A}{dV} + H_B\frac{dF_B}{dV} + \rho C_p\frac{dT}{dt}$$

The terms, $dF_A\frac{dH_A}{dV}$ and $dF_B\frac{dH_B}{dV}$ are so small compared to $F_A\frac{dH_A}{dV}$ and $F_B\frac{dH_B}{dV}$ that they can be neglected, hence it gives

(2.10) …… $$\frac{dQ}{dV} = F_A\frac{dH_A}{dV} + F_B\frac{dH_B}{dV} + H_A\frac{dF_A}{dV} + H_B\frac{dF_B}{dV} + \rho C_p\frac{dT}{dt}$$

As $\frac{dF_A}{dV} = r$ and $\frac{dF_B}{dV} = -r$

And $H_B - H_A = \Delta H_{rxn}$ (heat of reaction)

Also, $\frac{dH_A}{dV} = C_{PA}\frac{dT}{dV}$ and $\frac{dH_B}{dV} = C_{PB}\frac{dT}{dV}$

And, $\frac{dQ}{dV} = h\hat{a}\ (T_W - T)$

Where h is convection co-efficient between the wall of the reactor and the reacting fluid. T_w is the temperature of the wall and T is the temperature of the reacting fluid.

Substituting these in eq. (2.10), gives

$(F_A C_{PA} + F_B C_{PB})\frac{dT}{dV} + \rho C_p\frac{dT}{dt} = -\Delta H_{rxn} r + \frac{dQ}{dV}$

$\rho C_p\frac{dT}{dt} = - v_o \rho C_p \frac{dT}{dy} + \Delta H_{rxn} k_o \exp\left[\frac{-E_a}{RT}\right] C_A{}^n - h\hat{a}\ (T_W - T)$

Hence energy balance for the reacting fluid simplifies to,

(2.11) …… $\boldsymbol{\frac{dT}{dt} = - v_o \frac{dT}{dy} + \frac{(-\Delta H\ rxn)}{\rho Cp} k_o \exp\left[\frac{-E_a}{RT}\right] C_A{}^n - \frac{h\hat{a}}{\rho Cp}(T - T_w)}$

Boundary condition and initial condition –

As the PDE is first order in time and spatial dimension, one boundary condition and one initial condition were defined. Boundary condition of feed temperature at the inlet stays constant at the inlet feed temperature of the micro-channel was considered.

(B.C. 2) …… $T = T_f$ at $z = 0$

Initially, the fluid inside the micro-channel was at the fluid feed temperature at all points.

(I.C. 2) …… $T = T_{,f}$ at $t = 0$

Now for the wall, the energy balance considering heat flow from the streams to wall by convection and heat flow by conduction (K_w) in wall, gives

$$\textbf{(2.12) } \cdots\cdots\cdots\cdots \frac{dT_w}{dt} = \frac{1}{(\rho C_p)_w} [\, K_w \frac{\partial^2 T_w}{\partial z^2} + h\hat{a} (T - T_w) + q]$$

Where q is the constant heat flux from the heating coil with the units W/m^3

Boundary condition and initial condition –

As the PDE is first order in time and second order spatial dimension, two boundary condition and one initial condition were defined. Adiabatic boundary conditions were considered at the inlet and outlet points of the wall of the micro-channel. Considering the length of the micro-channel is discretized into 'n' equidistant parts,

(B.C. 3) …… $T_{w,0} = T_{w,1}$

(B.C. 4) …… $T_{w,\,n-1} = T_{w,n}$

Initially, the wall was at the fluid feed temperature at all points

(I.C. 3) …… $T_w = T_{,f}$ at $t = 0$

Hence, eqns. (2.5), (2.11) and (2.12) represent the mass and energy balance equations, B.C. 1, B.C. 2, B.C. 3, and B.C. 4 give the boundary conditions and I.C. 1, I.C. 2 and I.C. 3 give the initial condition for the model–

1. $\frac{dC_A}{dt} = -v_o \frac{dC_A}{dZ} - k_o \exp\left[\frac{-E_a}{RT}\right] C_A^n$

2. $\frac{dT}{dt} = -v_o \frac{dT}{dZ} + \frac{(-\Delta H\ rxn)}{\rho Cp} k_1 \exp\left[\frac{-E_a}{RT}\right] C_A^n - \frac{h\hat{a}}{\rho Cp}(T_w - T)$

3. $\frac{dT_w}{dt} = \frac{1}{(\rho C_p)_w}[K_w \frac{\partial^2 T_w}{\partial Z^2} + h\hat{a}(T - T_w) + q]$

2.2.3) Non- dimensionalization and parameter identification

The above equations were parameterized by defining the following dimensionless variables and parameters.

Dimensionless length s = $\frac{z}{L}$;

Residence time θ = $\frac{L}{v_o}$;

Dimensionless time = $\frac{t}{\theta}$;

Dimensionless concentration u = $\frac{C_A}{C_{A,f}}$; where $C_{A,f}$ is the inlet concentration of the reactant

Adiabatic temperature $T_{ad} = \frac{C_{A,f}(\Delta H)_{rxn}}{(\rho C_p)}$

Dimensionless reacting fluid temperatures v = $\frac{T - T_f}{T_{ad} - T_f}$;

Dimensionless wall temperatures $v_w = \frac{T_w - T_f}{T_{ad} - T_f}$;

Dimensionless Activation energy α = $\frac{E_a}{RT_f}$;

This resulted in the identification of six governing dimensionless groups.

- Fourier Number, Fo = $\frac{K_w \theta}{L^2 (\rho C_p)_w}$
- Solid phase axial conduction parameter, CP = $\frac{K_w \theta}{L^2 (\rho C_p)}$
- Damkohler Number, Da = $k_o exp\left[\frac{-E_a}{RT_f}\right] (C_{A,f})^{n-1} \theta$
- Adiabatic temperature rise, $\gamma = \frac{T_{ad} - T_f}{T_f}$
- Number of transfer units (Frank P., 2011), NTU = $\frac{h\hat{a}\theta}{(\rho C_p)}$
- External heating parameter, psi, $\Psi = \frac{L^2 q}{K_w \gamma T_f}$

The Damkohler number, Fourier number, Number of Transfer Units, and Solid phase axial conduction parameter; all contain residence time, which will be later defined as the 'disturbance' for the controls section of this research. Hence, for controls analysis, residence time was extracted from each of these four dimensionless groups and represented as –

- $Da = Da^*. \theta$ (Da^* is dictated only by reaction kinetics)
- $Fo = Fo^*. \theta$ (Fo^* is dictated by the dimension and material properties of the wall)
- $NTU = NTU^*. \theta$ (NTU^* is dictated by the thermal and material properties of the flow and wall)
- $CP = CP^*. \theta$ (CP^* is dictated by the dimension and material properties of the flow and wall)

As noted above, for the controls analysis of this research, residence time, θ, is considered as the disturbance. The dimensionless heating rate, ψ, is considered the control variable and the conversion (X), which is (1-u) per the dimensionless parameters defined earlier, is the process variable. Hence the dimensionless mass balance and energy balance equations become,

$$\textbf{(2.13)} \ldots\ldots\ldots\ldots \frac{\partial u}{\partial \tau} = -\frac{\partial u}{\partial s} - \boldsymbol{Da} *. \theta \, \boldsymbol{exp}\left[\frac{\alpha\gamma v}{1+\gamma v}\right](\boldsymbol{u})^{\boldsymbol{n}}$$

$$\textbf{(2.14)} \ldots\ldots\ldots\ldots \frac{\partial v}{\partial \tau} = -\frac{\partial v}{\partial s} + \boldsymbol{Da} \ *. \theta \boldsymbol{exp}\left[\frac{\alpha\gamma v}{1+\gamma v}\right](\boldsymbol{u})^{\boldsymbol{n}} - \boldsymbol{NTU} *. \theta[\boldsymbol{v} - \boldsymbol{v_w}]$$

$$\textbf{(2.15)} \ldots\ldots\ldots\ldots \frac{\partial v_w}{\partial \tau} = \boldsymbol{Fo} *. \theta \frac{\partial^2 v_w}{\partial s^2} + \boldsymbol{Fo}\left\{\frac{\boldsymbol{NTU}*}{\boldsymbol{CP}*}[\boldsymbol{v_w} - \boldsymbol{v}] + \ \boldsymbol{\psi}\right\}$$

At steady state, the equations reduce to

$$\textbf{(2.16)} \ldots\ldots\ldots\ldots \frac{\partial u}{\partial s} = -\boldsymbol{Da} *. \theta \, \boldsymbol{exp}\left[\frac{\alpha\gamma v}{1+\gamma v}\right](\boldsymbol{u})^{\boldsymbol{n}}$$

$$\textbf{(2.17)} \ldots\ldots\ldots\ldots \frac{\partial v}{\partial s} = \boldsymbol{Da} \ *. \theta \boldsymbol{exp}\left[\frac{\alpha\gamma v}{1+\gamma v}\right](\boldsymbol{u})^{\boldsymbol{n}} - \boldsymbol{NTU} *. \theta[\boldsymbol{v} - \boldsymbol{v_w}]$$

$$\textbf{(2.18)} \ldots\ldots\ldots\ldots \frac{\partial^2 v_w}{\partial s^2} = -\left\{\frac{\boldsymbol{NTU}}{\boldsymbol{CP}}[\boldsymbol{v_w} - \boldsymbol{v}] + \ \boldsymbol{\psi}\right\}$$

2.3) Parameter estimation

2.3.1) Introduction

To investigate the effect of material of construction of micro-reactor, reaction kinetics and geometry; the dimensionless groups' values were calculated. Nine different materials were considered for building the micro-reactor with a range of values of material density and specific heat.

2.3.2) Operating conditions for micro reactor made of SS316

Table 1 presents the general design data and operating conditions for the micro-channel system. The dimensions for the micro-channel are taken as those used experimentally by (Kundu, 2006) where a square conduit is considered of size 0.3mm x 0.2mm and a length of 37mm. The catalyst used is Pd/ZnO which is wall coated. A total of 40 micro-channels are considered in one micro-reactor block. The heat required for the reaction is provided by an external heater which transmits heat through the wall of the micro-channel. An inlet temperature of 290˚C is considered for the incoming methanol and steam. Table 2 presents the data of the constants from literature.

Table 1 – Flow rate calculations

	Water	**Methanol**	**Units**
Feed flow rate	0.005		ml/min
Molar ratio	2	1	
Density	1000	793	kg/m^3
Combined flow Density	931		kg/m^3
Mol. wt.	18	32	g/mol
Combined mol. wt.	22.67		g/mol
Feed flow rate	3.42E-06		ml/sec

Table 2 – Parameter values for calculations

R (gas constant)	8.314	$Jmol^{-1}K^{-1}$
K (Cao, 2003)	2.91E+10	
E_A (Behrens & Armbruster, 2012)	94800	J/mol
p_{MeOH}	3.33E-01	Atm
p_{H2O}	6.67E-01	Atm
Catalyst density (Kundu, 2006)	900	kg/m^3
Thickness of cat (Kundu, 2006)	0.025	Mm
Open volume	1.78E-09	m^3
Vol ratio cat/channel	0.198	m^3cat/m^3
K_w (Cverna, 2002)	16	J/msK
Density wall	8000	kg/m^3
Cp,w	500	J/kg.K
Heat of reaction	49700	J/mol
Cp,air	1000	J/kg.K
Density of air	1	kg/m^3
h (conv btwn wall &fluid) (Cverna, 2002)	11.3	W/m^2K

To calculate residence time, we consider ideal gas assumptions as temperature is sufficiently high and pressure is low. The calculation is presented in table 3 –

Table 3 – Residence time calculations

Parameter	Value	Units
Volumetric flow rate	1.58E-07	m^3/sec
Velocity/Channel	6.60E-02	m/sec
Residence Time	5.60E-01	sec

2.3.3) Material defined parameters – CP, Fo

For conducting the study of effect of material of construction of micro-reactor channel, different materials were considered which have been listed in table 1 (Cverna, 2002). Based on the combination of their Fo^* and CP^* values, stainless Steel 316 (low Fo^* and low CP^*), Silicon (intermediate Fo^* and intermediate CP^*) and Copper (high Fo^* and high CP^*) were chosen to perform the studies to cover a broad spectrum of effect of material of construction on MSR reaction control in a micro-channel reactor.

On completion of material selection, literature was surveyed for finding good values for the other dimensionless groups. In the paper by (Kundu, 2006); experiments were carried out using a stainless steel 316 micro reactor and a heating plate for uniform heating rate. Table 4 presents the different materials considered for building the micro-reactor.

Table 4 – Fo^* and CP^* values for different materials of build for micro-channel reactor

Material	Density (kg/m^3)	C_p (J/kgK)	K (J/m.s.K)	Fo^*	CP^*
SS316	8000	500	16	0.002922	11.7323
Copper	8940	384	400	0.085111	293.3074
Aluminum	2800	904	235	0.067817	172.3181
SS304	7700	502	16	0.003024	11.7323
CS	7850	502	47	0.008712	34.46362
Alumina	3950	880	18	0.003783	13.19883
Silicon	2330	710	150	0.066233	109.9903
PBI	1300	930	0.41	0.000248	0.30064
Inconel	8440	460	14.1	0.002653	10.33909

2.3.4) Kinetics defined parameters – Da, $\Delta T_{ad,}$ α

The Damkohler number is calculated using the rate expression presented by eq. (2.19) (Cao, 2003).

(2.19) …… $-r_A$ (mmol/kg_{cat}/s) = 2.9047 x 10^{10} e $^{-94800/RT}$ $p_{MeOH}^{0.715}$ p_{H20} $^{0.088}$

Where r_A is rate of the reaction, p_{MeOH} is the partial pressure of methanol and p_{H20} is the partial pressure of water. Kinetics calculations and NTU calculations are presented in table 5 and table 6 respectively.

Table 5 – Kinetics based dimensionless number calculation

	Value	**Units**
Rate wrt. catalyst	8.36E+02	mmol/kgcat.s
Rate	1.49E+02	$mol/m^3.s$
Reference conc.	7.215674646	$molCH_3OH/m^3$
Da*	**20.6**	**1/s**
ΔT_{ad}	**-358.62**	**K**
γ	**-0.673**	
α	**20.25**	

2.3.5) Geometry and material defined parameters – NTU, Ψ

Table 6 – NTU Calculations

	Value	**Units**
Perimeter	1.00E-03	m^2
Area for conv.	1.67E+04	m^{-1}
NTU*	**1.88E+02**	**1/s**

Heating rate calculations are presented in table 7.

Table 7 – Dimensionless heating rate Calculations

	Value	**Units**
Flow/channel	2.85233E-08	mol/sec
Reaction heat	1.42E-03	J/s
q	6.39E+05	W/m^3
Ψ	**-1.52E-01**	

Feed flow rate ranged between **0.05 ml/ min to 0.5ml/min** in the paper by (Kundu, 2006); which results in residence time range of **0.56 sec to 0.056 sec.** The dimensionless parameters for the 3 materials selected to be studied in this research are tabulated in table 8.

Table 8 – Dimensionless parameters for different materials

Parameters/ Material	**SS316**	**Cu**	**Si**
Fo*	0.002922	0.08511	0.06623
CP*	11.73	293.3	110
Da*	20.6	20.6	20.6
NTU*	188	188	188
Ψ	-0.152	-0.0061	-0.016
γ	-0.673	-0.673	-0.673

The conversion of methanol achieved experimentally at a temperature of 290 ˚C, (Kundu, 2006) ranged from 98% for a feed flowrate of 0.05 ml/min and a conversion of 52% when a flowrate of

0.5 ml/min was used. In the subsequent section, MATLAB R2016a ® simulation was used to validating the mathematical model for this model and effects of flowrate, material and heating rate was studied to find the optimal conditions to study the controllability of each material.

2.4) Mathematical modelling

2.4.1) Finite Difference Method (FDM)

Finite difference method (Grossman, 2007) is a mathematical method to simplify solving differential equations by estimating them as difference equations. The derivative is approximated as finite differences (Olver, 2013). Hence, finite difference method is classified as a discretization method. The approximation for finite difference method is done using a Taylor series expansion (Grewal, 2008). Using the Taylor series expansion, a first order derivative with respect to 'z' at any point 'a' can be represented as –

(2.20) …… $\frac{\partial u}{\partial z} = \frac{u(a+\Delta z)-u(a)}{\Delta z}$

Similarly, a second order derivative with respect to 'z' at any pint 'a' can be represented as –

(2.21) …… $\frac{\partial^2 u}{\partial z^2} = \frac{u(a+\Delta z)-2u(a)+u(a-\Delta z)}{\Delta z^2}$

The errors associated with using a finite difference method arise because of rounding off error (Ueberhuber, 1997) and discretization error (Higham, 2002).

- **Rounding Errors** – The loss of precision owing to a computer program rounding of the decimals for every step in space.
- **Discretization Error** – Because of making a continuous function into a finite number of difference equations, error creeps in based on the size of each step.

Smaller each step is, less is the error. But making the step size very small results in a proportional increase in the number of difference equations the computer has to solve and hence increases the run-time for the program.

2.4.2) Modelling of system of partial differential equations using FDM

The system of partial differential equations (eqns. 2.13, 2.14 and 2.15) for simulating methanol steam reforming reaction is a micro-channel reactor was formulated using eqns. 2.22, 2.23 and 2.24 as –

(2.22) ..... $\frac{\partial u}{\partial \tau} = -\frac{u(i)-u(i-1)}{\Delta z} - Da^*.\theta\, exp\left[\frac{\alpha\gamma v\,(i-1)}{1+\gamma v(i-1)}\right]\left(u(i-1)\right)^n$

(2.23) ..... $\frac{\partial v}{\partial \tau} = -\frac{v(i)-v(i-1)}{\Delta z} + Da^*.\theta\ \ exp\left[\frac{\alpha\gamma v(i-1)}{1+\gamma v(i-1)}\right]\left(u(i-1)\right)^n - NTU^*.\theta\,[v(i-1) - v_w(i-1)]$

(2.24) ..... $\frac{\partial v_w}{\partial \tau} = Fo^*.\theta\frac{v_w(i+1)-v_w(i-1)+\,2\,v_w(i)}{(\Delta z)^2} + Fo^*.\theta\left\{\frac{NTU}{CP}[v_w(i) - v(i)] + \ \psi\right\}$

Boundary conditions for the discretized model are –

u(0) = 1 (from B.C. 1)

v(0) = 0 (from B.C. 2)

v_w (0) = v_w (1) (from B.C. 3)

v_w (N) = v_w (N-1) (from B.C. 4)

And the initial conditions for the discretized model are –

u (@ all points at t=0) = 1 (from I.C. 1)

v (@ all points at t=0) = 0 (from I.C. 2)

v_w (@ all points at t=0) = 0 (from I.C. 3)

An evenly distributed grid with 200 discretization points was chosen as the grid size for the simulations based on trial and error. Discretization points were increased till there was less than 0.1% difference between the data obtained by doubling the discretization points. MATLAB R2016a ® was used to simulate these equations, the ode23s solver was used to solve this system of equations. Ode 23s is good for solving stiff differential equations.

For initial simulations, a 'cold start-up' for the reaction was simulated considering initial dimensionless concentration and initial dimensionless stream temperature throughout the micro-channel as 0. The open loop (Distefano, Stubberud, & Williams, 1967) dynamic simulation results are shared in the forthcoming chapter. The MATLAB codes are attached in the annexures.

CHAPTER III

OPEN LOOP SIMULATION

3.1) Introduction

An open loop system is one in which the output has no effect on the input signal. In an open loop system, no information is being fed back from the output to the input of the system hence the system is not able to take any corrective action when the system starts deviating from the set point, regardless of the final output.

In this chapter, open loop simulations have been carried out for the methanol steam reforming reaction in micro-channel reactors made of made of SS316 (in section 3.3), Copper (in section 3.4) and Silicon (in section 3.5). The PDE model is validated by comparing the results that were achieved experimentally at (Kundu, 2006). The dynamic responses for start-up and step changes have been investigated for all the 3 materials. A 90% outlet conversion for methanol was taken as the set point for our process variable after consulting literature. Finally, a state space (algebraic) model was derived for the process variable with dependence on control variable and disturbance.

3.2) Model validation

Considering a mesh size of 200 spatial discretization (Δz) along the length of a micro-channel, simulations were carried out to observe the variation of outlet conversion of methanol and outlet temperatures of reacting stream and wall for the micro-channel reactor made of SS316.

Fig. 5(a) shows the unsteady state change in outlet conversion for methanol with respect to time and fig. 5(b) shows the unsteady state change in temperatures of the outlet stream and wall outlet

with respect to time for a residence time of 0.056 seconds for a time span of 7000 seconds, till it reaches a steady state in a stainless steel 316 micro-channel reactor. A cold start-up is considered as the initial condition of the micro-channel reactor and a constant heating rate of 640 kW/m^3 is provided through the wall.

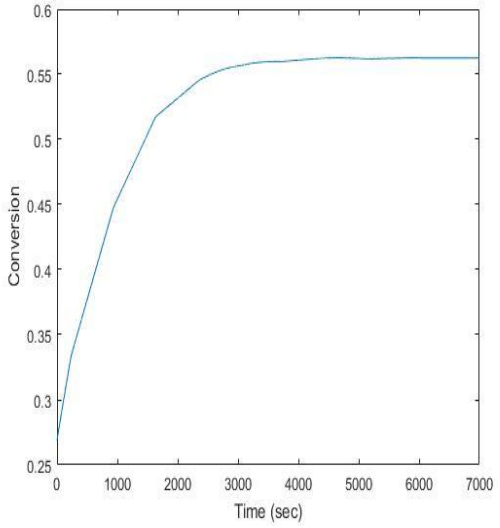

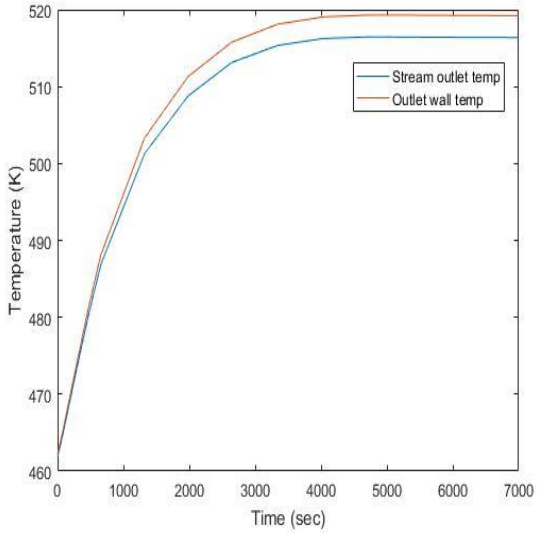

Fig. 5(a) – Unsteady state outlet conv vs time (SS)

Fig. 5(b) – Unsteady state temp vs time (SS)

Fig. 6(a) shows the steady state change in conversion along the length of a micro-channel and fig. 6(b) shows the steady state change in temperatures of the stream and wall along the length of a micro-channel for a residence time of 0.056 seconds in a stainless steel 316 micro-channel reactor. Under the same conditions and process parameters, the outlet conversion for methanol achieved experimentally by (Kundu, 2006), was 52%.

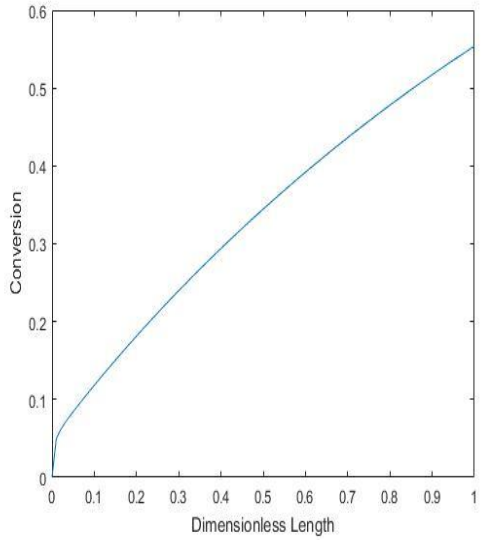

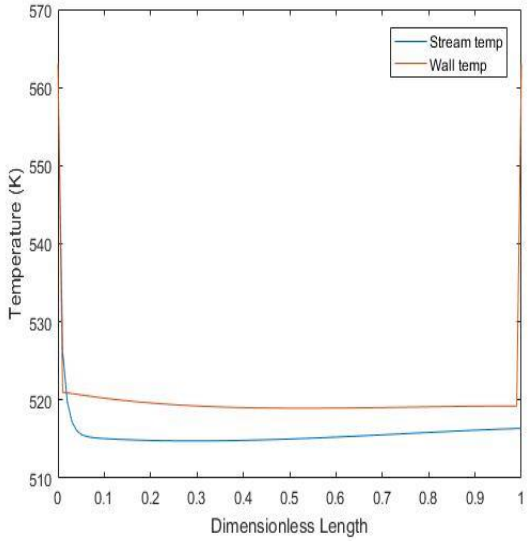

Fig. 6(a) – Conversion along the micro-channel

Fig. 6(b) – Temperature along the micro-channel

3.3) Open loop simulations for SS316

Simulations were carried out for different flow rates, which was considered as the disturbance, and different heating rates, which was considered as the controlled variable in the controls section of this research. A contour plot of steady state outlet conversion with respect to residence time and heating rate is presented in fig. 7. As a reference, a ψ value of -0.1 corresponds to a heating rate of 418.6 kW/m^{3}and a ψ value of -0.05 corresponds to a heating rate 209.3 kW/m^3. The outlet conversion contour here represents the conversion value of methanol at the outlet, on reaching steady state after starting up the micro-channel reactor with a cold start-up (Verwijs, 1995).

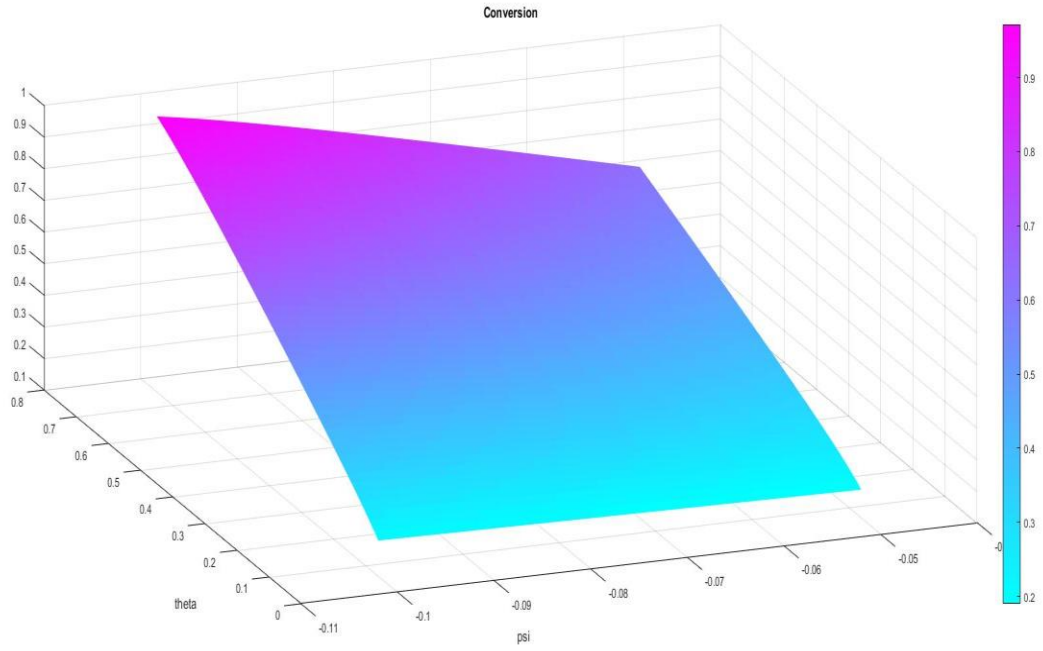

Fig. 7 – Contour plot of steady state outlet conversions with respect to residence time and heating rate in SS316

An outlet conversion for methanol of 90 % at steady state was identified as the target for the controls section of this research. A turn-down ratio (Smith & L., Practical Process Control Tuning and Troubleshooting, 2009) (ratio between the maximum and minimum value) of 4 was considered for the residence time, varying between 1.4 seconds to 0.35 seconds. For a micro-channel system, this range of heating rate is optimal and provides ample room for controllability of the system.

Simulations were run to find the plot line of 90 % outlet conversion of methanol for the range of residence times between 0.35 seconds to 1.4 seconds by adjusting the value of the heating rate. To study the effect of step changes on control of the system, simulations were carried to study the dynamics of the outlet conversion and heating rate for different size of step increases and decreases

of heating rate. A plot line curve of the 90 % outlet conversion of methanol in a SS316 micro-channel along with the different step changes are shown in fig. 8.

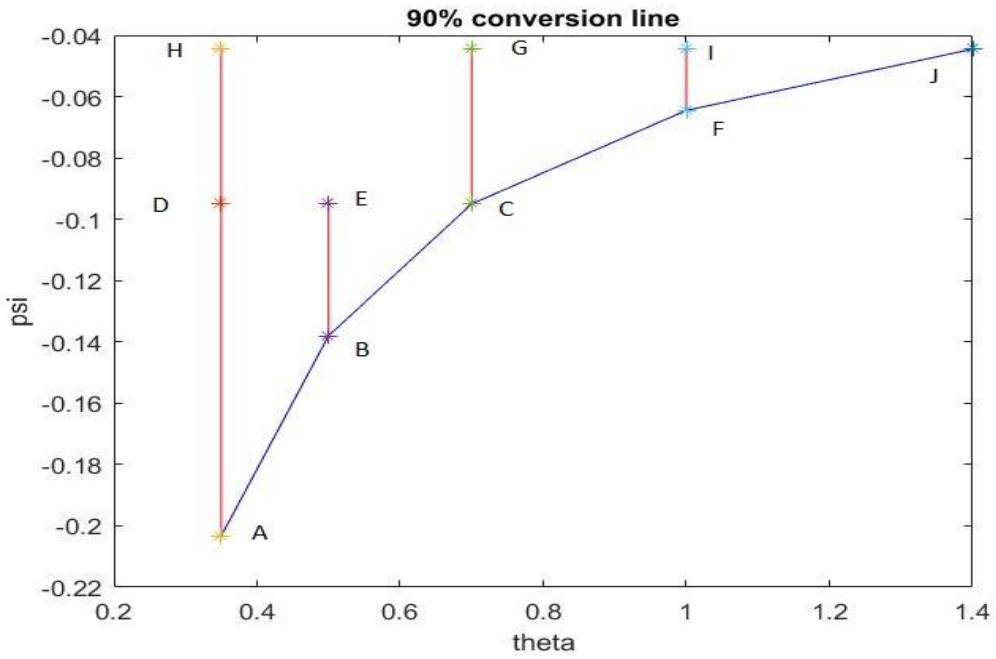

Fig. 8 – 90% outlet conversion of methanol in SS316

The dynamic state change in outlet conversion and stream and wall temperature were plotted using MATLAB R2016a ® and the plots were approximated as depicting first order characteristics by using the cftool toolbox on MATLAB R2016a ®. Eq. 3.1 represents a first order model.

(3.1) …… $(t) = A * K * (1 - exp\frac{(-t)}{\tau})$

Where, A → Step size

K → Steady State Gain

τ → Time constant

Table 9(a), 9(b) and 9(c) represents the parameters of the estimated first order model for outlet methanol conversion, stream outlet temperature wall temperature at inlet respectively as achieved from the cftool toolbox.

Table 9(a) – Outlet conv. of Me, parameter assumption using first order model for SS

	Step Size	Steady State Gain	Time Constant	R-square	Error % from perfect FO
A->D	-0.1038	3.4	752	0.9991	0.09
D->A	0.1038	3.366	633.8	0.9999	0.01
C->G	-0.0505	6.671	718.1	0.999	0.1
G->C	0.0505	6.591	605	0.9999	0.01
A->H	-0.1588	3.275	730	0.9993	0.07
H->A	0.1588	3.259	659.6	0.9998	0.02
B->E	-0.043	4.622	771	0.9991	0.09
E->B	0.043	4.564	652.1	0.9998	0.02
F->I	-0.02	9.47	752	0.9991	0.09
I->F	0.02	9.307	637.4	0.9998	0.02
Average			**691.1**		**0.052**

Table 9(b) – Outlet stream temp, parameter assumption using first order model for SS

	Step Size	Steady State Gain	Time Constant	R-square	Error % from perfect FO
A->D	-0.1038	0.8573	647.35	0.9999	0.01
D->A	0.1038	0.8549	784.3	1	0
C->G	-0.0505	1.498	620.2	0.9999	0.01
G->C	0.0505	1.488	730.4	1	0
A->H	-0.1588	0.7977	656.3	1	0
H->A	0.1588	0.7979	776.6	1	0
B->E	-0.043	1.21	669	0.9999	0.01
E->B	0.043	1.202	784.8	1	0
F->I	-0.02	2.241	655.1	0.9999	0.01
I->F	0.02	2.213	750.9	1	0
Average			**707.495**		**0.004**

Table 9(c) – Inlet wall temp, parameter assumption using first order model for SS

	Step Size	Steady State Gain	Time Constant	R-square	Error % from perfect FO
A->D	-0.1038	0.6231	672.6	1	0
D->A	0.1038	0.6192	677.1	0.9998	0.02
C->G	-0.0505	1.22	645.5	0.9999	0.01
G->C	0.0505	1.211	673.5	0.998	0.2
A->H	-0.1588	0.6118	702	1	0
H->A	0.1588	0.6098	657.7	0.9998	0.02
B->E	-0.043	0.8837	678.7	0.9999	0.01
E->B	0.043	0.87	721.7	0.9998	0.02
F->I	-0.02	1.87	665.8	0.9999	0.01
I->F	0.02	1.844	721.4	0.9999	0.01
Average			**681.6**		**0.03**

These values of steady state gain and time constant were used later in the controls section of the research.

To simplify the design of the controller and to make the simulations faster, an approximate model of outlet conversion (the process variable in the control section of this research) was derived with respect to residence time and dimensionless heating rate. After trial and error using the cftool toolbox, an algebraic relationship (Swaney & Rawlings, 2014) was derived for estimating the steady state conversion for a range of values residence times ranging from 0.35 seconds to 1.4 seconds and corresponding values of dimensionless heating rates to achieve outlet methanol conversions in the range of 40% - 90%. The algebraic relationship (approximate function) was found to be of the form –

(3.2) …… $X = A*\theta + B*\psi + C*\psi*\theta + D$

Where, X is the outlet conversion and A, B, C and D are constants which depend on the material of build of the micro-channel reactor. Table 10(a) shows the values of steady state outlet methanol conversion using the actual PDE model and table 10(b) shows the corresponding values using the approximate model. The values of constants A, B, C and D for the case of SS316 are –

A	**0.116**
B	**-0.196**
C	**-9.32**
D	**0.18**

Table 10(a) – Outlet methanol conversion using PDE model

Theta / *Psi*	0.35	0.6125	0.875	1.1375	1.4
-0.052	0.4023	0.5624	0.7152	0.8605	0.9832
-0.0527	0.4048	0.5669	0.7217	0.8684	0.9888
-0.0535	0.4073	0.5714	0.7281	0.8763	0.9933
-0.0543	0.4098	0.5759	0.7345	0.8841	0.9966
-0.055	0.4123	0.5804	0.7409	0.8919	0.9986
-0.0575	0.4206	0.5955	0.7622	0.9171	
-0.06	0.4289	0.6105	0.7833	0.9411	
-0.0625	0.4373	0.6255	0.8043	0.9632	
-0.065	0.4456	0.6405	0.8251		
-0.0675	0.454	0.6555	0.8456		
-0.07	0.4624	0.6704	0.8659		
-0.0725	0.4708	0.6854	0.8858		
-0.075	0.4792	0.7003	0.9052		
-0.0775	0.4876	0.7151			
-0.0906	0.5318	0.7923			
-0.1038	0.5761	0.8669			
-0.1169	0.6204	0.936			
-0.13	0.6645	0.9892			
-0.135	0.6813				
-0.165	0.7805				
-0.195	0.8753				
-0.225	0.9588				
-0.255	0.9996				

Table 10(b) – Outlet methanol conversion using approximate model and error % compared to PDE model

Theta / *Psi*	0.35	0.6125	0.875	1.1375	1.4
-0.052	0.400416	0.558084	0.715752	0.87342	1.031088
-0.0527	0.402837	0.562217	0.721598	0.880978	1.040359
-0.0535	0.405603	0.566941	0.728279	0.889616	1.050954
-0.0543	0.408369	0.571664	0.734959	0.898254	1.061549
-0.055	0.41079	0.575798	0.740805	0.905813	1.07082
-0.0575	0.419435	0.590559	0.761683	0.932806	
-0.06	0.42808	0.60532	0.78256	0.9598	
-0.0625	0.436725	0.620081	0.803438	0.986794	
-0.065	0.44537	0.634843	0.824315		
-0.0675	0.454015	0.649604	0.845193		
-0.07	0.46266	0.664365	0.86607		
-0.0725	0.471305	0.679126	0.886948		
-0.075	0.47995	0.693888	0.907825		
-0.0775	0.488595	0.708649			
-0.0906	0.533895	0.785998			
-0.1038	0.57954	0.863937			
-0.1169	0.62484	0.941286			
-0.13	0.67014	1.018635			
-0.135	0.68743				
-0.165	0.79117				
-0.195	0.89491				
-0.225	0.99865				
-0.255	1.10239				
Error %	1.076785	0.918927	0.080256	1.722437	5.92768
Avg. Error%	**1.28**				

In the controls section of this research, both approximate and PDE model were used to study the effect on response of the system. In section 3.4 and 3.5, similar open loop studies have been

represented for copper and silicon micro-channel reactors respectively to study the impact of material of build of micro-channel reactor on the open loop response of the system.

3.4) Open loop simulation results for Copper

Considering a mesh size of 200 spatial discretization (Δz) along the length of a micro-channel, simulations were carried out to observe the variation of outlet conversion of methanol and outlet temperatures of reacting stream and wall for the micro-channel reactor made of copper.

Fig. 9(a) shows the unsteady state change in outlet conversion for methanol with respect to time and fig. 9(b) shows the unsteady state change in temperatures of the outlet stream and wall outlet with respect to time for a residence time of 0.056 seconds for a time span of 5000 seconds, till it reaches a steady state in a copper micro-channel reactor. A cold start-up is considered as the initial condition of the micro-channel reactor and a constant heating rate of 640 kW/m^3 is provided through the copper wall.

The steady state conversion and temperature profiles along the length of the micro-channel reactor made of copper are identical to that observed in fig. 6(a) and fig. 6(b) for a SS316 micro-channel reactor.

Similarly, simulations were carried out for different flow rates, which was considered as the disturbance, and different heating rates, which was considered as the manipulated variable in the controls section of this research. A contour plot of steady state outlet conversion with respect to residence time and heating rate is presented in fig. 10. As a reference, a ψ value of -0.004 corresponds to a heating rate of 418.6 $kW/m^3$and a ψ value of -0.002 corresponds to a heating rate

209.3 kW/m^3. The outlet conversion contour here represents the outlet conversion value of methanol on reaching steady state after starting up the micro-channel reactor with a cold start-up.

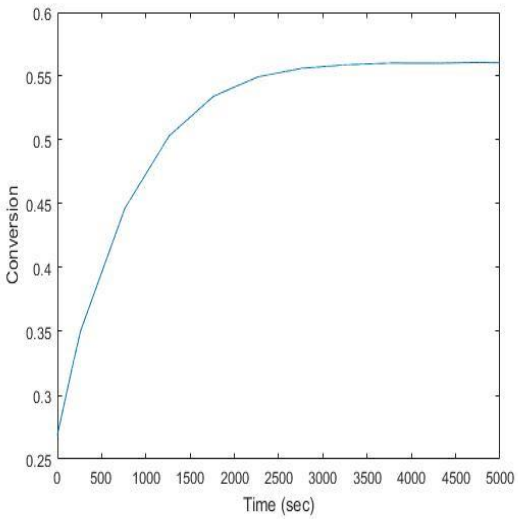

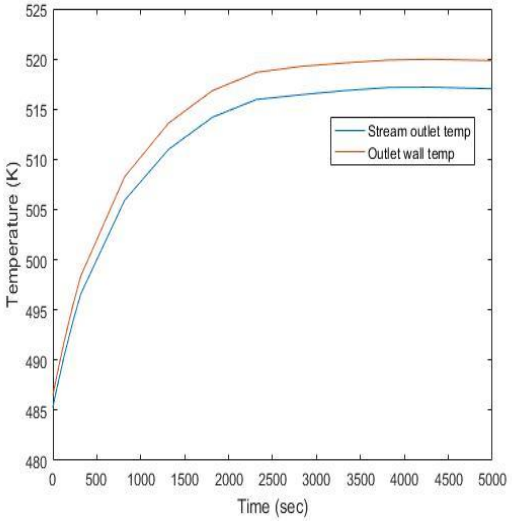

Fig. 9(a) – Unsteady state outlet conv vs time (Cu)

Fig. 9(b) – Unsteady state temp vs time (Cu)

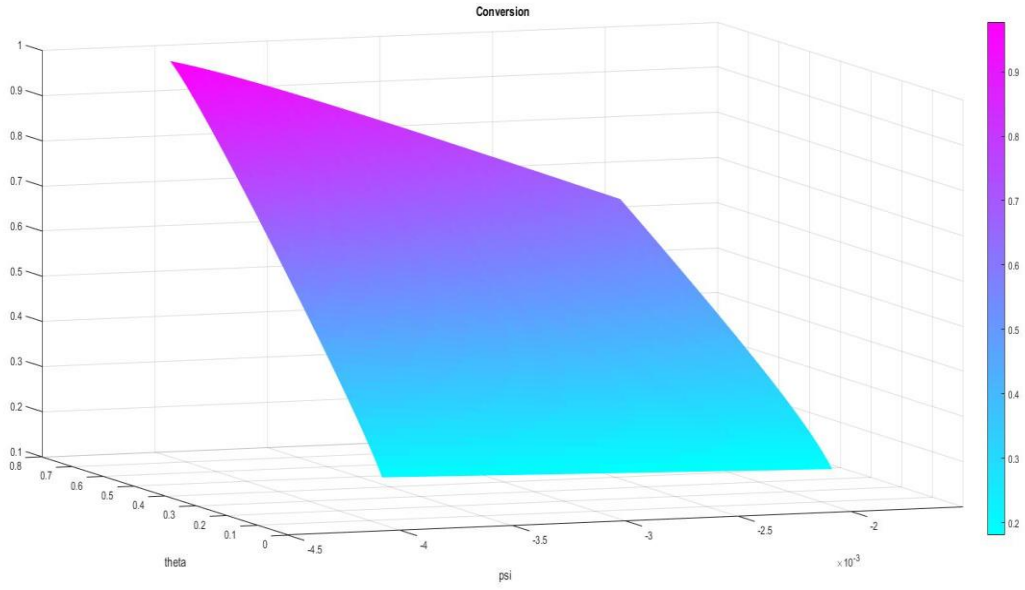

Fig. 10 – Contour plot of steady state outlet conversions with respect to residence time and heating rate in Cu

Like section 3.3, an outlet conversion for methanol of 90% at steady state was identified as the target for the controls section of this research and a turn-down ratio of 4 was considered for the residence time, varying between 1.4 seconds to 0.35 seconds.

Simulations were run to find the plot line of 90% outlet conversion of methanol for the range of residence times between 0.35 seconds to 1.4 seconds by adjusting the value of the heating rate. To study the effect of step changes on control of the system, simulations were carried to study the dynamics of the outlet conversion and heating rate for different size of step increases and decreases of heating rate. A plot line curve of the 90% outlet conversion of methanol in a copper micro-channel along with the different step changes are shown in fig. 11.

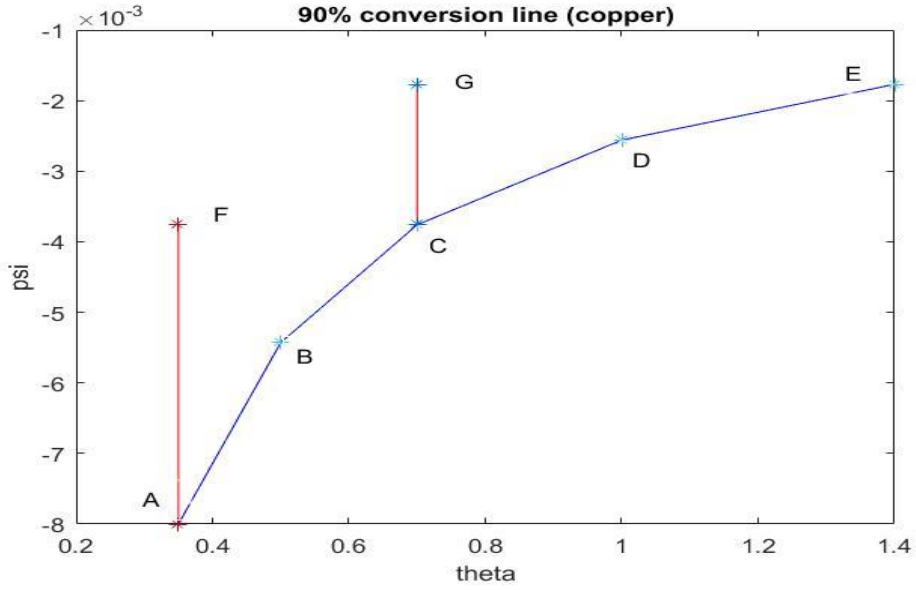

Fig. 11 – 90% outlet conversion of methanol in Cu

The dynamic state responses were approximated as showing first-order characteristics (Powell, 2004), as found by using the cftool toolbox on MATLAB R2016a ®. The values for system gain

and time constant for the outlet conversion of methanol, outlet stream temperature and inlet wall temperature are tabulated in table 11(a), 11(b) and 11(c) respectively.

Table 11(a) – Outlet conv of Me, parameter assumption using first order model for Cu

	Step Size	Steady State Gain	Time Constant	R-square	Error % from perfect FO
A->F	-0.00424	79.09	637.7	0.9968	0.32
F->A	0.00424	80.82	538.5	0.9993	0.07
C->G	-0.00199	135.5	447.3	0.9552	4.48
G->C	0.00199	139.1	446.7	0.9889	1.11
Average			**517.55**		**1.495**

Table 11(b) – Outlet stream temp, parameter assumption using first order model for Cu

	Step Size	Steady State Gain	Time Constant	R-square	Error % from perfect FO
A->F	-0.00424	17.91	560	0.9974	0.26
F->A	0.00424	18.1	628.7	0.9987	0.13
C->G	-0.00199	29.1	402.2	0.9666	3.34
G->C	0.00199	25.98	517.4	0.9818	1.82
Average			**527.075**		**1.3875**

Table 11(c) – Inlet wall temp, parameter assumption using first order model for Cu

	Step Size	Steady State Gain	Time Constant	R-square	Error % from perfect FO
A->F	-0.00424	17.4	582.7	0.997	0.3
F->A	0.00424	17.58	611.3	0.999	0.1
C->G	-0.00199	28.44	404.9	0.9653	3.47
G->C	0.00199	27.07	478.9	0.9846	1.54
Average			**519.45**		**1.3525**

The approximate model for the outlet conversion of methanol with respect to residence time and dimensionless heating rate was given by the eq. 3.2 in section 3.1 and the corresponding values of the constants for copper can be given as –

A	**0.1234**
B	**-7.81**
C	**-230.9**
D	**0.17**

The error percentage on using the approximate model as compared to the actual PDE model was found to 1.5%.

3.5) Open loop simulation results for Silicon

Considering a mesh size of 200 spatial discretization (Δz) along the length of a micro-channel, simulations were carried out to observe the variation of outlet conversion of methanol and outlet temperatures of reacting stream and wall for the micro-channel reactor made of silicon.

Fig. 12(a) shows the unsteady state change in outlet conversion for methanol with respect to time and fig. 12(b) shows the unsteady state change in temperatures of the outlet stream and wall outlet with respect to time for a residence time of 0.056 seconds for a time span of 3000 seconds, till it reaches a steady state in a silicon micro-channel reactor. A cold start-up is considered as the initial condition of the micro-channel reactor and a constant heating rate of 640 kW/m^3 is provided through the silicon wall. The steady state conversion and temperature profiles along the length of the micro-channel reactor made of silicon are identical to that observed in fig. 5(a) and fig. 5(b) for a SS316 micro-channel reactor. Similarly, simulations were carried out for different flow rates,

which was considered as the disturbance, and different heating rates, which was considered as the manipulated variable in the controls section of this research.

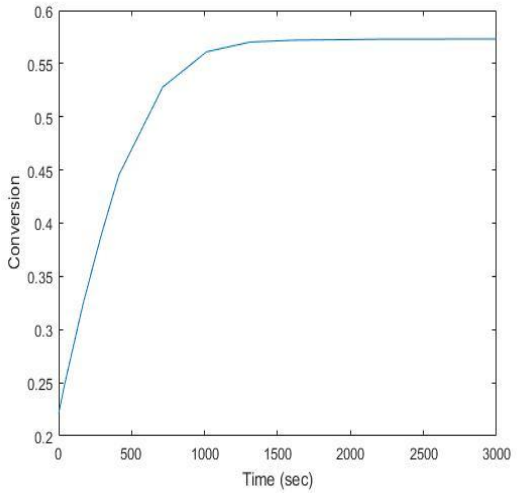

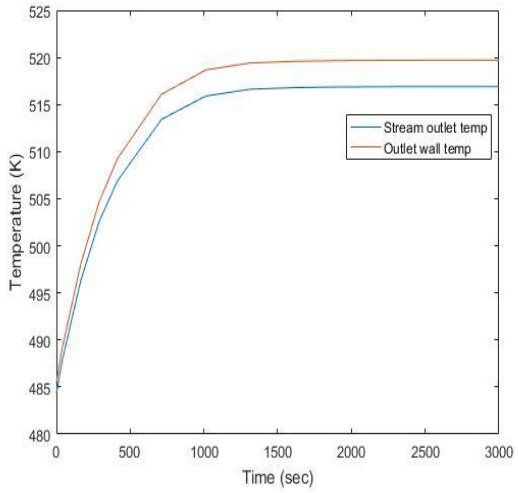

Fig. 12(a) –Unsteady state outlet conv vs time (Si) **Fig. 12(b)** – Unsteady state temp vs time (Si)

A contour plot of steady state outlet conversion with respect to residence time and heating rate is presented in fig. 13. As a reference, a ψ value of -0.004 corresponds to a heating rate of 418.6 $kW/m^3$and a ψ value of -0.002 corresponds to a heating rate 209.3 kW/m^3. The outlet conversion contour here represents the outlet conversion value of methanol on reaching steady state after starting up the micro-channel reactor with a cold start-up.

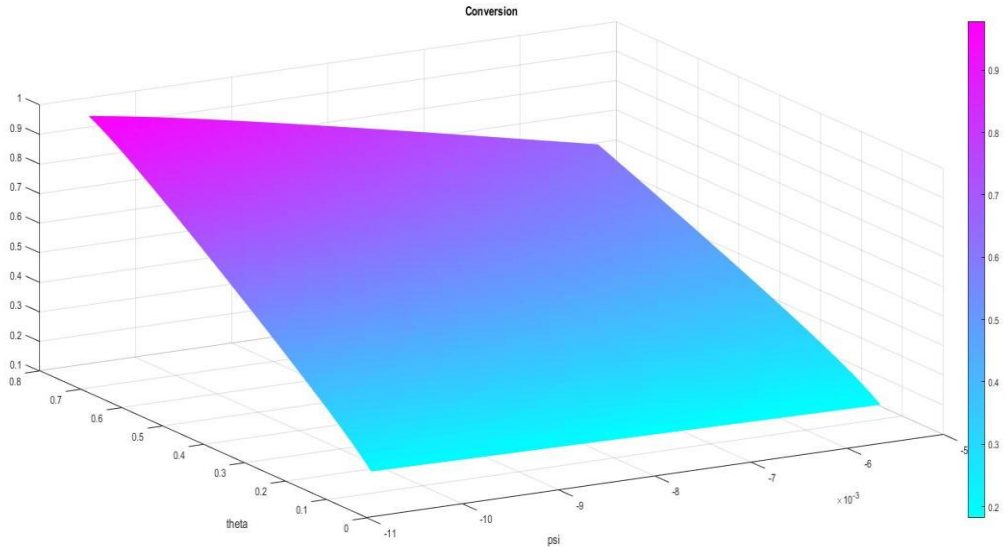

Fig. 13 – Contour plot of steady state outlet conversions with respect to residence time and heating rate in Si

Like section 3.3, an outlet conversion for methanol of 90% at steady state was identified as the target for the controls section of this research and a turn-down ratio of 4 was considered for the residence time, varying between 1.4 seconds to 0.35 seconds.

Simulations were run to find the plot line of 90% outlet conversion of methanol for the range of residence times between 0.35 seconds to 1.4 seconds by adjusting the value of the heating rate. To study the effect of step changes on control of the system, simulations were carried to study the dynamics of the outlet conversion and heating rate for different size of step increases and decreases of heating rate. A plot line curve of the 90% outlet conversion of methanol in a silicon micro-channel along with the different step changes are shown in fig. 14.

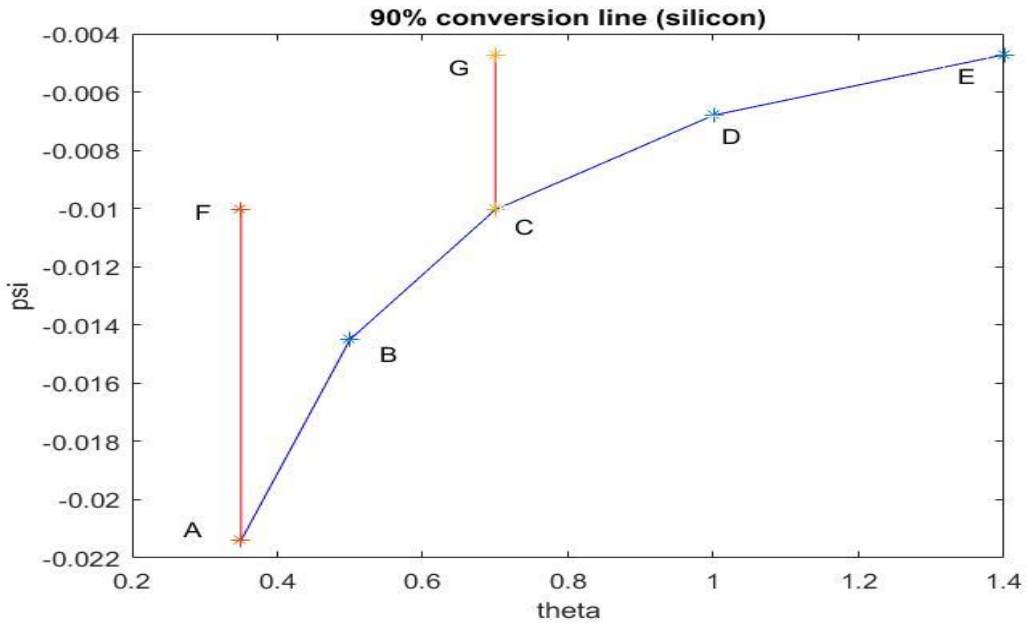

Fig. 14 – 90% outlet conversion of methanol in Si

The dynamic state responses were approximated as showing first-order characteristics, as found by using the cftool toolbox on MATLAB R2016a ®. The values for system gain and time constant for the outlet conversion of methanol, outlet stream temperature and inlet wall temperature are tabulated in table 12(a), 12(b) and 12(c) respectively.

Table 12(a) – Outlet conv of Me, parameter assumption using first order model for Si

	Step Size	Steady State Gain	Time Constant	R-square	Error % from perfect FO
A->F	-0.01136	31.45	328.6	0.9986	0.14
F->A	0.01136	30.99	268.2	0.9999	0.01
C->G	-0.00532	60.47	279.9	0.9831	1.69
G->C	0.00532	63.4	257.1	0.9987	0.13
Average			**283.45**		**0.4925**

Table 12(b) – Outlet stream temp, parameter assumption using first order model for Si

	Step Size	Steady State Gain	Time Constant	R-square	Error % from perfect FO
A->F	-0.01136	7.154	278.3	0.9991	0.09
F->A	0.01136	7.075	315	0.9999	0.01
C->G	-0.00532	12.76	245	0.9869	1.31
G->C	0.00532	13.38	307.8	0.9978	0.22
Average			**286.525**		**0.4075**

Table 12(c) – Inlet wall temp, parameter assumption using first order model for Si

	Step Size	Steady State Gain	Time Constant	R-square	Error %
A->F	-0.01136	6.776	289.2	0.9988	0.12
F->A	0.01136	6.709	304.4	0.9999	0.01
C->G	-0.00532	12.33	251.1	0.9854	1.46
G->C	0.00532	12.91	267	0.9967	0.33
Average		**9.68125**	**277.925**		**0.48**

The approximate model for the outlet conversion of methanol with respect to residence time and dimensionless heating rate was given by the eq. xxxi in section 4.1 and the corresponding values of the constants for silicon can be given as –

A	**0.1177**
B	**-2.413**
C	**-85.2**
D	**0.18**

The error percentage on using the approximate model as compared to the actual PDE model was found to 1.1%.

3.6) Observations from open loop simulations

1. The response time depends on the material of construction of the micro-channel reactor by a factor of the thermal capacity of the wall (Fourier number (Fo) / Solid phase axial Conduction Parameter (CP)). Lesser the ratio, quicker is the response. In this study, SS316 has the highest ratio (4015), Silicon has the lowest (1660) and Copper has an intermediate ratio (3446).
2. For all the 3 materials (SS316, Cu, Si), starting up with the same process parameters (heating rate and flowrate), they reach the same steady state eventually. Just the time to reach the steady state varies based on the material of construction of the micro-channel.
3. All dynamic responses (outlet methanol conversion, outlet stream temperature, inlet wall temperature) approximate to a first order response with non-linearity (the non-linearity can be attributed to the different gain values for the different step sizes) (Hinrichsen D, 2005).
4. The steady state outlet conversion can be approximated as an algebraic equation as, $\mathbf{X = A*\theta + B*\psi + C*\psi*\theta + D}$**, where** A, B, C and D are material dependent.

CHAPTER IV

PROCESS CONTROL WITH APPROXIMATE MODEL

4.1) Introduction

In this chapter, the state space model (algebraic relation) developed in the previous chapter was used in a closed loop with a PI controller and the system response characteristics were studied. The effect of material of build of micro-reactor on the control of the system was investigated. Two types of control problems were investigated for this research – Servo problem (set point change in outlet conversion) and regulator problem (Variation in the disturbance). The effect of changing the proportional gain on the settling time for the system was also investigated in detail. Section 4.2 discusses the selection of PI controller with a Hammerstein model which had been selected to compensate for the non-linearity of the first order model. Section 4.3, 4.4 and 4.4 show the simulation results for servo and regulator problems for micro-channel reactors made of SS316, Copper and Silicon respectively. In Section 4.6, the control results of the 3 different materials were compared.

4.2) Controller selection

A first order system is best controlled by using a Proportional Integral (PI) controller (Astrom, 2002). A proportional (P) controller shows overshoot, a long settling time and a steady state error. The Integral (I) controller has more overshoot than the proportional controller due to the slowness of the starting of the integral behavior. Also, the integral (I) controller has a longer settling time than a P controller but doesn't produce any steady-state error. The PI controller integrates the properties of P and I controllers where the overshoot and settling time are like the P controller but

it doesn't give any steady state error. A derivative (D) action is not required for first order models. Because of having a nonlinear state space model for conversion, a PI controller with a Hammerstein model (Nelles, 2001) is considered. A Hammerstein model can be described as a cascaded system with a non-linear block preceding a linear block (Wills, 2012). This model assumes that there is a separation between the nonlinearity section and the dynamics of the process. Fig. 15 depicts a block diagram of a first order system with a PI controller with a Hammerstein Model. A state space model is considered for the first part of the controls study in this research (Hangos & R. Lakner, 2001). Considering the outlet conversion (X) of methanol in the micro-channel as the controlled variable, the heating rate (ψ) as the manipulated variable and residence time (θ) as the disturbance; the PI controller was used in a closed loop by using the Hammerstein model to implement feedback control.

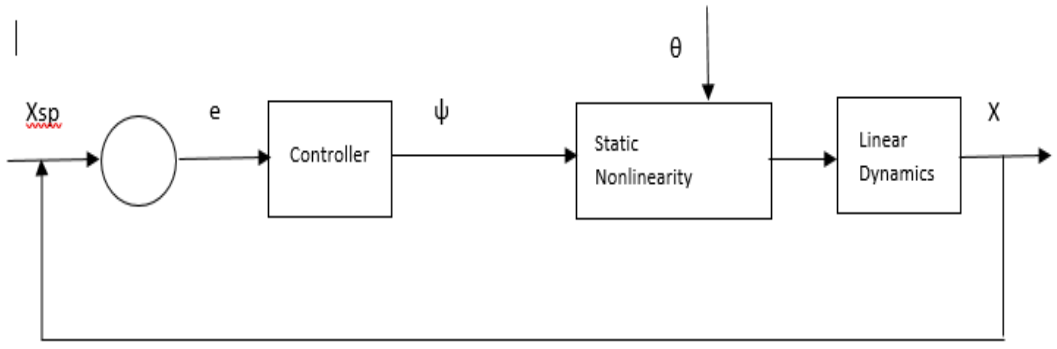

Fig. 15 – Block diagram of a first order systems with a PI controller with Hammerstein model

The equation for the closed loop is given by eqns. 4.1, 4.2 and 4.3.

(4.1) …… $\tau \frac{\partial X}{\partial t}$ + X = (A θ + B ψ + C θ ψ + D)

where τ is the time constant of the system (Ogunnaike, 1994).

(4.2) …… $\psi = \psi_b + K_c\left(E_p + \frac{e}{\tau i}\right)$

where ψ_b is the bias heating rate (the heating rate at the initial steady state)

e is the integral error

τ_i is the integral time of the PI controller

(4.3) …… $E_p = Xsp - X$

X_{sp} is the set point for conversion which is 0.9 (90% outlet methanol conversion) for most of the simulation in this research.

The integral error for the PI controller closed loop is given by the differential equation shown in eq. 4.4.

(4.4) …… $\frac{\partial e}{\partial t} = Xsp - X$

The settling time (Ogata, 2010) is normally defined as the time required to reach within 2%-5% of the final value. In this study, for more accurate control, settling time was taken as the maximum of time required to reach 0.5% of the set point value or the time required for the change in conversion (slope) to be between 0.1 and 0.0001. The controller parameters for proportional gain (k_c) and integral time (τ_i) are adjustable. Their effect on control quality on the micro-channel system have been studied in this research.

Two types of control problems were investigated in this study –

a) **Servo problem** – The objective is to guide the system to follow the changes in set point (Ogunnaike, 1994). In this study, this was achieved by changing the set point for conversion, when system was at an original steady state and examining the controller dynamic response to reach of the subsequent steady state.

b) **Regulator problem** – The objective is to apply corrective action to make the system return to the set point when perturbed from it due to a disturbance. Regulator problems require effective disturbance rejection capability (Ogunnaike, 1994). In this study, this was achieved by changing the flow rate and examining the controller dynamic response to return to the set point.

In the sections 4.3, 4.4 and 4.5, servo and regulator problems are simulated for the methanol steam reforming reaction in a micro-channel reactor made of SS316, copper and silicon respectively by using the state space representation (approximate conversion model) with PI controller in a closed loop. Sections 5.2, 5.3 and 5.4; then present the same studies by using the actual PDE model and compares the veracity of both the models.

4.3) Closed loop simulations for MSR in SS316 micro-channel reactor with state space model

4.3.1) Servo problem – Step up

The step up servo problem studied for this research was with a set point change of outlet conversion from 56% to 90%. The integral time was taken as the time constant for open loop response (τ_i = 700 seconds for SS316). The proportional gain was varied and the effect on system response for outlet conversion, heating rate and change in heating rate was studied.

Fig. 16 shows the effect of proportional gain on the settling time for conversion and the heating rate.

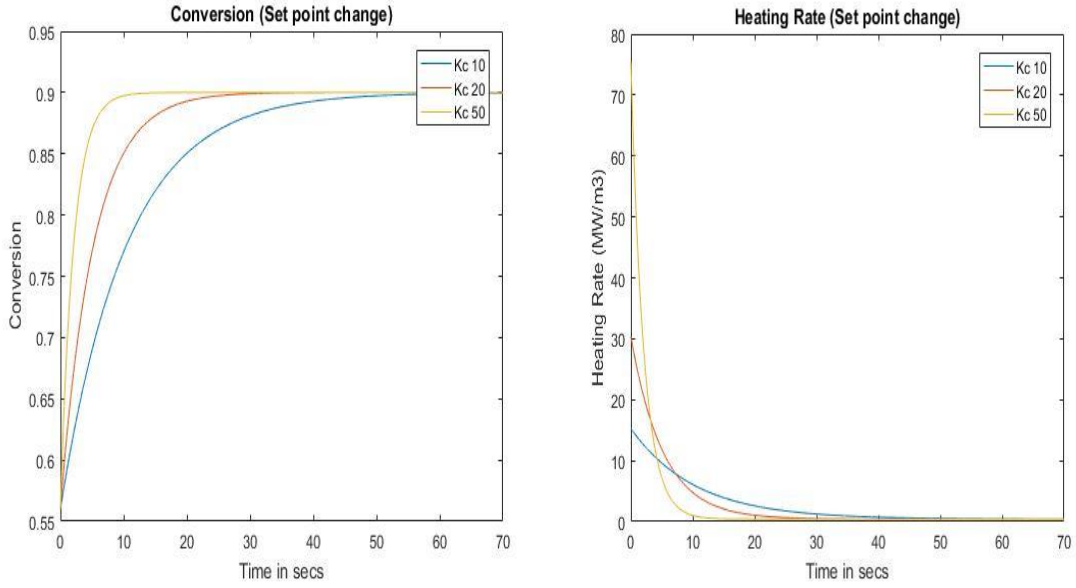

Fig 16 – Conversion and heating rate plots for different K_c values for a set point change from 56% to 90% on conversion in a SS316 micro-channel reactor

As observed from the plots, increasing the proportional gain results in faster control but also requires higher heating rates. From literature (Kawamura, Ogura, & Igarashi, 2013), a heater with maximum heat flux of 35 MW/m^3 is achievable in a micro-channel reactor. Table 13 presents the results for control action using a PI controller. An achievable settling for a SS316 micro- channel reactor with a maximum heating rate of **35 MW/m^3 is 32.3 seconds**. Fig. 17 presents a log-log plot of Maximum heating flux versus settling time for the servo problem.

Table 13 –Heating rate response with PI controller in a SS316 micro-channel reactor

τ_i	K_c	Settling Time (s)	Maximum Heating flux (MW/m^3)	Maximum rate of change of heating flux (MW/m^3s)
700	10	68.48	15.1	1.2
700	**25**	**31.78**	**37.5**	**7.6**
700	50	13.42	74.8	30.3
700	100	6.08	149.4	121.4
700	150	5.18	224.0	273.1
700	200	4.85	298.7	485.4
700	300	3.31	447.9	1091.5

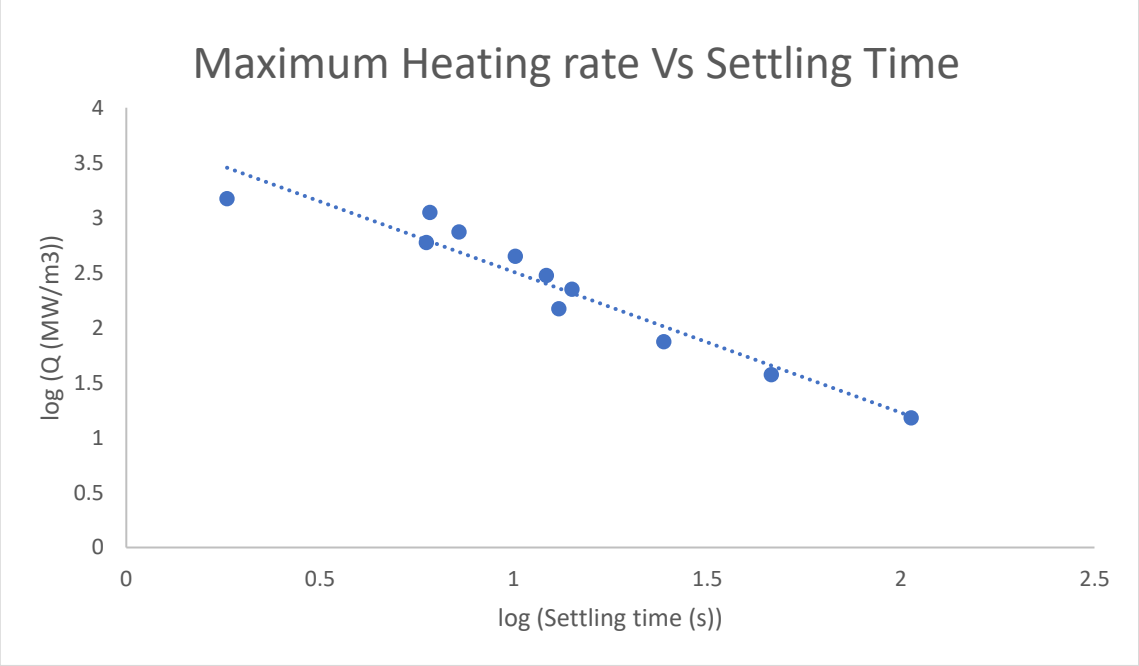

Fig. 17- Log-log plot of max heating rate vs settling time with a PI controller in SS

4.3.2) Servo problem – Step down

The step-down servo problem studied for this research was with a set point change of outlet conversion from 90% to 85%. The integral time was taken as the time constant for open loop response (τ_i = 700 seconds for SS316). The proportional gain was varied and the effect on system response for outlet conversion, heating rate and change in heating rate was studied.

Fig. 18 shows the effect of proportional gain on the settling time for conversion and the heating rate.

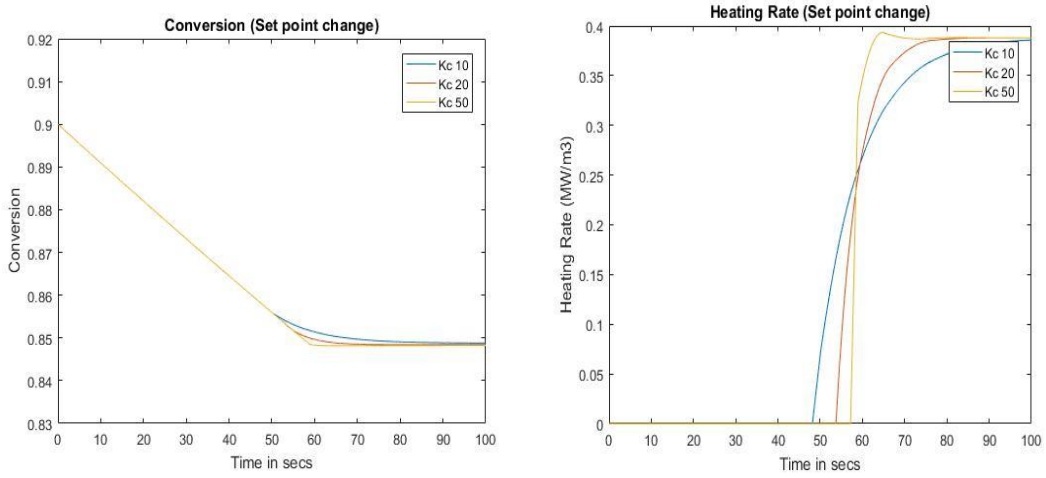

Fig 18 – Conversion and heating rate plots for different K_c values for a set point change from 90% to 85% on conversion in a SS316 micro-channel reactor

As can be observed from the heating rate plot in fig. 18, the heater shuts down at the set point step down and starts up per the value of the proportional gain. Higher the proportional gain, later the heater turns back on. Also, the conversion profiles coincide in the initial timespan for all the three different values of proportional gain which can be justified as the heater is off in that timespan in all the three cases. The settling time observed in the step-down servo problem doesn't depend strongly on the proportional gain used in the controller.

4.3.3) Regulator problem

The regulator problem studied for this research was with a change in disturbance (residence time) from 0.35 seconds to 0.7 seconds. The system was initially at an outlet conversion of 90% and the objective was to study the response of the model to keep the system at 90% outlet conversion when the residence time was increased. The integral time was taken as the time constant for open loop response (τ_i = 700 seconds for SS316). The proportional gain was varied and the effect on system response for outlet conversion, heating rate and change in heating rate was studied.

Fig. 19 shows the effect of proportional gain on the settling time for conversion and the heating rate. For the regulator problem for step up in residence time, the maximum heating rate is not a constraint. Only important parameter here was to consider that the heater didn't start acting like a cooler for faster control.

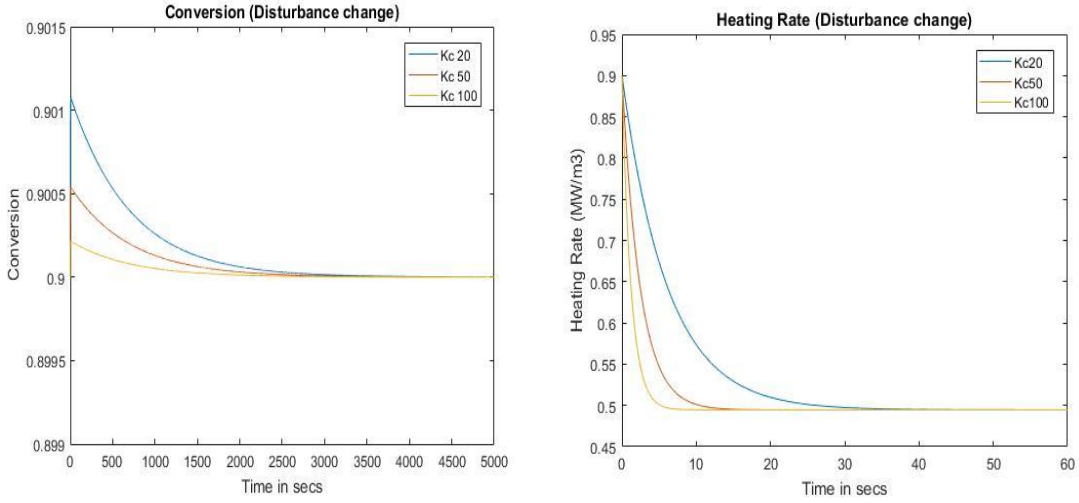

Fig 19 – Conversion and heating rate plots for different K_c values for a residence time change from 0.35 secs to 0.7 secs on conversion in a SS316 micro-channel reactor

As can be observed from the heating rate plot in fig. 18, maximum heating rate is always the highest at initial time of the step change, hence the only criteria to define the effectiveness of the control is the speed of response of the heater, faster the change in heating rate, faster will be the control for the system. Table 14 presents the results for control action using a PI controller for the reduction in flow rate. Fig. 20 presents a log-log plot of Maximum rate of change of heating flux versus settling time for the regulator problem.

Table 14 – **Max change in heating rate response in a SS316 micro-channel reactor**

τ_i	**Kc**	**Settling time (s)**	**Maximum rate of change of heating flux (MW/m^3s)**
700	10	48.89	0.033
700	25	28.79	0.0812
700	50	15.7	0.162
700	100	7.26	0.315
700	150	6.54	0.460
700	200	3.92	0.598
700	300	2.49	0.854
700	500	2.23	1.296
700	1000	1.06	2.100

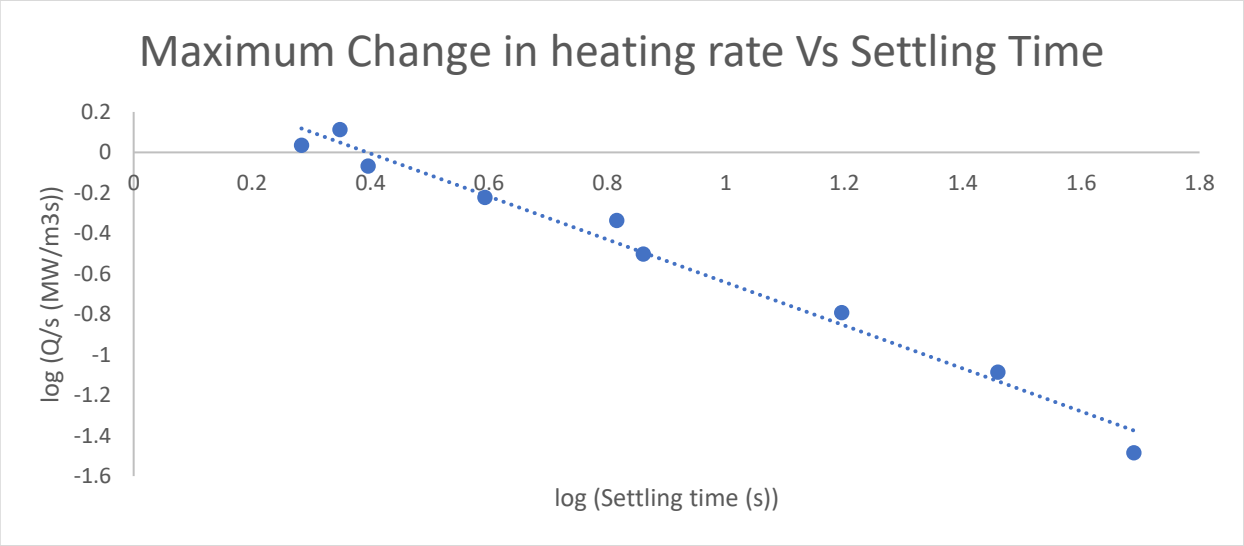

Fig. 20- log-log plot of max change in heating rate vs settling time with a PI controller in SS

4.4) Closed loop simulations for MSR in Copper micro-channel reactor with state space model

4.4.1) Servo problem

Like the case of stainless steel 316, the servo problem for micro-channel reactor made of Copper investigated the effect of a PI controller for control of the state-space model when a set point change was made from 56% to 90% on the outlet conversion of methanol. The integral time was taken as the time constant for open loop response (τ_i = 500 seconds for Copper). The proportional gain was varied and the effect on system response for outlet conversion, heating rate and change in heating rate was studied. Fig. 21 shows the effect of proportional gain on the settling time for conversion and the heating rate. Like in section 4.3.1; increasing the proportional gain results in faster control but also requires higher heating rates.

Table 15 presents the results for control action using a PI controller. An achievable settling time for a copper micro- channel reactor with a maximum heating rate of **35 MW/m^3 is 23.1 seconds**.

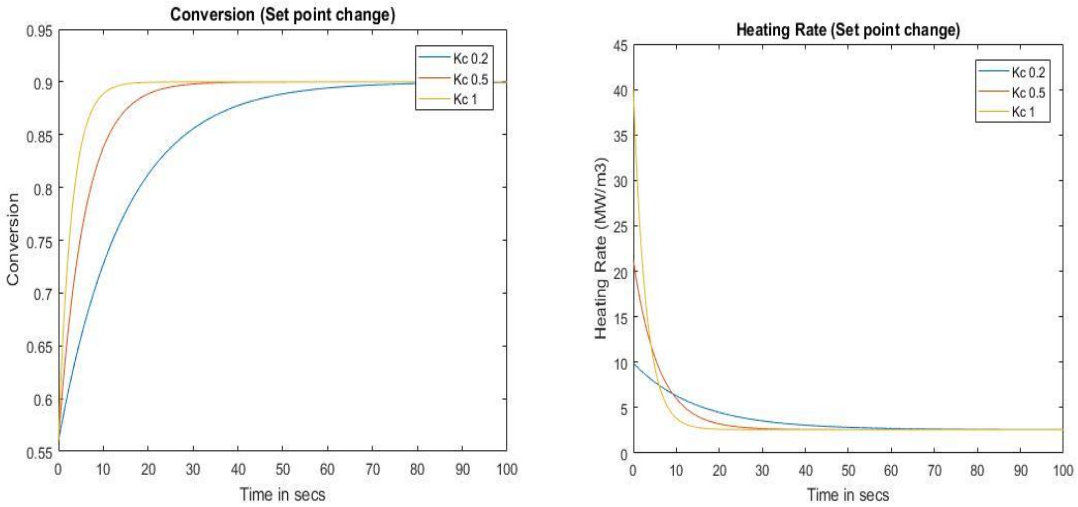

Fig. 21 – Conversion and heating rate plots for different K_c values for a set point change from 56% to 90% on conversion in a Copper micro-channel reactor

Table 15 – **Heating rate response with PI controller in a Copper micro-channel reactor**

τ_i	K_c	Settling Time (s)	Maximum Heating flux (MW/m^3)	Maximum rate of change of heating flux (MW/m^{3}s)
500	0.1	153.71	0.4	0.1
500	0.5	39.7	20.4	3.1
500	1	21.85	37.6	12.5
500	2	11.73	75.0	50.1
500	5	7.17	187.2	313.4
500	10	3.5	374.3	1252.3
500	25	1.21	935.4	7804.4
500	50	1.08	1871.2	31106.7

Fig. 22 presents a log-log plot of Maximum heating flux versus settling time for the servo problem.

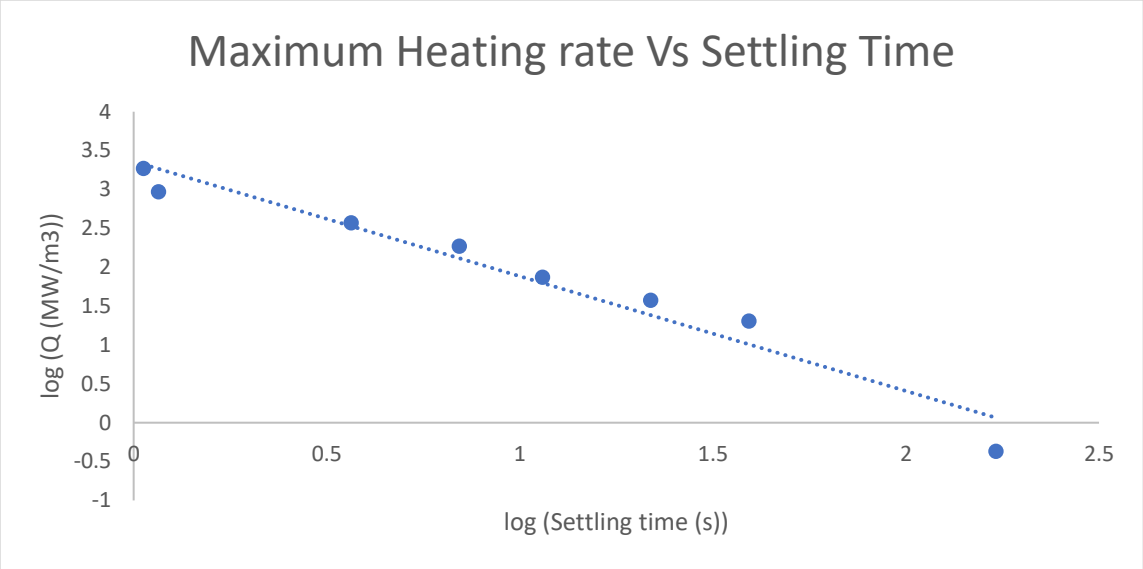

Fig. 22- Log-log plot of max heating rate vs settling time with a PI controller in Cu

4.4.2) Regulator problem

Like in section 4.3.3, the regulator problem studied for this research was with a change in disturbance (residence time) from 0.35 seconds to 0.7 seconds. The integral time was taken as the time constant for open loop response (τ_i = 500 seconds for Copper). The proportional gain was varied and the effect on system response for outlet conversion, heating rate and change in heating rate was studied. Fig. 23 shows the effect of proportional gain on the settling time for conversion and the heating rate.

As can be observed from the heating rate plot in fig. 23, maximum heating rate is always the highest at initial time of the step change, hence the only criteria to define the effectiveness of the control is the speed of response of the heater, faster the change in heating rate, faster will be the control for the system. Table 16 presents the results for control action using a PI controller for the

reduction in flow rate. Fig. 24 presents a log-log plot of Maximum rate of change of heating flux versus settling time for the regulator problem.

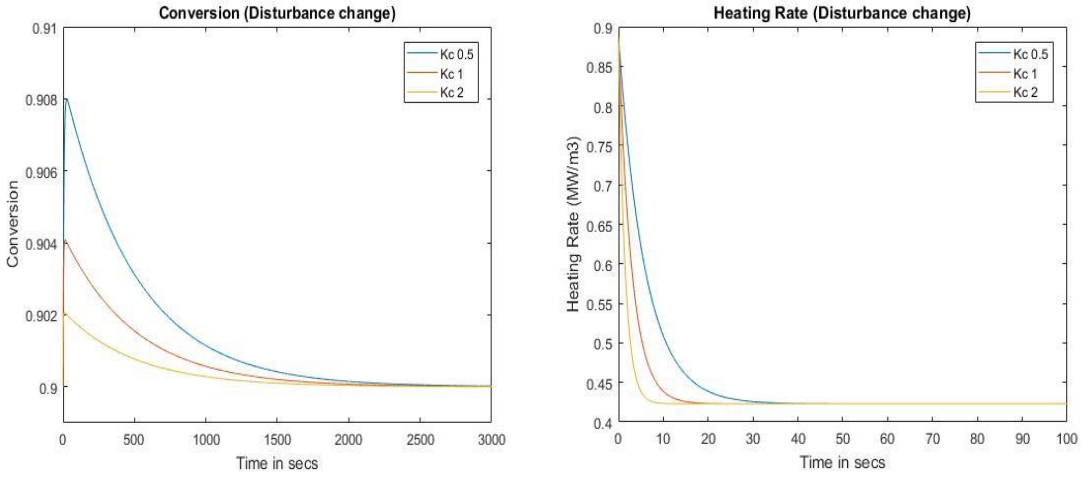

Fig 23 – Conversion and heating rate plots for different K_c values for a residence time change from 0.35 secs to 0.7 secs on conversion in a Copper micro-channel reactor

Table 16 – **Max change in heating rate response in a Copper micro-channel reactor**

τ_i	Kc	Settling time (s)	Maximum rate of change of heating flux (MW/m^3s)
500	1	7.5	0.2
500	2	5.09	0.3
500	5	2.56	0.7
500	10	1.28	1.3
500	25	0.68	2.7
500	50	0.45	4.1
500	75	0.1	4.9
500	100	0.54	5.3
500	150	0.54	5.7

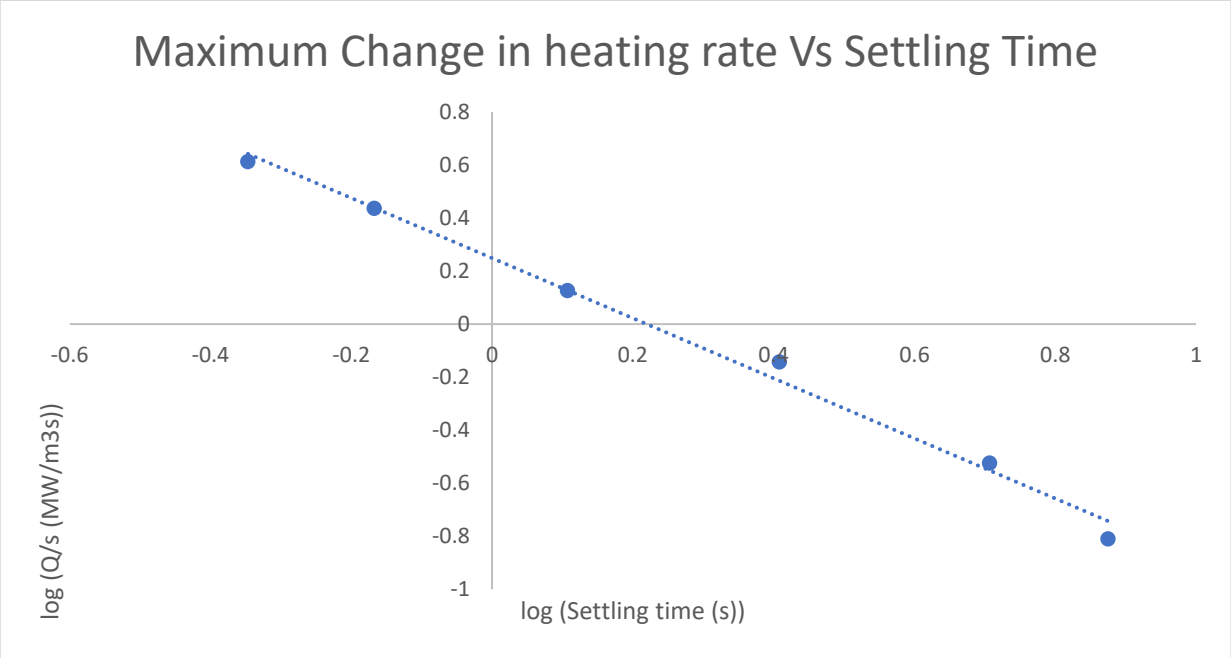

Fig. 24 - log-log plot of max change in heating rate vs settling time with a PI controller in Cu

4.5) Closed loop simulations for MSR in Silicon micro-channel reactor with state space model

4.5.1) Servo problem

Like the case of stainless steel 316 and copper in sections 4.3.1 and 4.4.1 respectively, the servo problem for micro-channel reactor made of Silicon investigated the effect of a PI controller for control of the state-space model when a set point change was made from 56% to 90% on the outlet conversion of methanol. The integral time was taken as the time constant for open loop response (τ_i = 300 seconds for Silicon). The proportional gain was varied and the effect on system response for outlet conversion, heating rate and change in heating rate was studied. Fig. 25 shows the effect of proportional gain on the settling time for conversion and the heating rate. Like in section 5.3.1

and 4.4.1; increasing the proportional gain results in faster control but also requires higher heating rates.

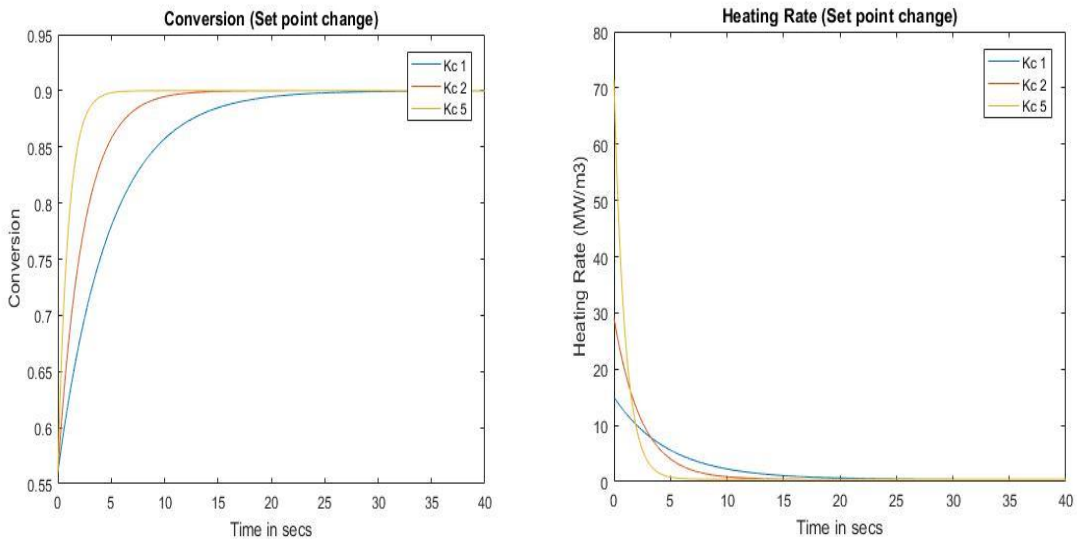

Fig. 25 – Conversion and heating rate plots for different K_c values for a set point change from 56% to 90% on conversion in a Silicon micro-channel reactor

Table 17 presents the results for control action using a PI controller. An achievable settling time for a copper micro- channel reactor with a maximum heating rate of **35 MW/m^3 is 14.3 seconds**. Fig. 26 presents a log-log plot of Maximum heating flux versus settling time for the servo problem.

Table 17 – Heating rate response with PI controller in a Silicon micro-channel reactor

τ_i	K_c	Settling Time (s)	Maximum Heating flux (MW/m^3)	Maximum rate of change of heating flux (MW/m^3s)
300	1	32.21	14.2	0.0675
300	2	17.29	28.3	0.2722
300	5	7.36	70.4	1.7079
300	10	4.54	140.5	6.8347
300	25	2.43	351.0	42.6527
300	50	1.33	701.8	170.1824
300	100	1.27	1403.4	678.1054
300	150	1.31	2105.0	1521.1

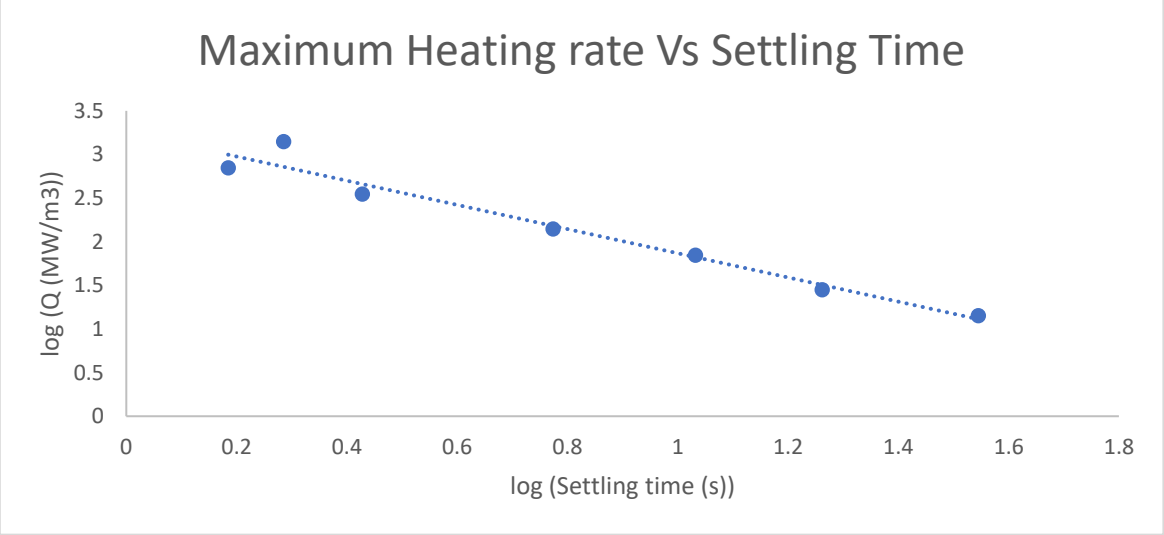

Fig. 26 - Log-log plot of max heating rate vs settling time with a PI controller in Si

4.5.2) Regulator problem

Like in section 4.3.3 and 4.4.2 for SS316 and Copper, the regulator problem studied for this research was with a change in disturbance (residence time) from 0.35 seconds to 0.7 seconds. The integral time was taken as the time constant for open loop response (τ_i = 300 seconds for Silicon). The proportional gain was varied and the effect on system response for outlet conversion, heating rate and change in heating rate was studied.

Fig. 27 shows the effect of proportional gain on the settling time for conversion and the heating rate. As can be observed from the heating rate plot in fig. 27, maximum heating rate is always the highest at initial time of the step change, hence the only criteria to define the effectiveness of the control is the speed of response of the heater, faster the change in heating rate, faster will be the control for the system. Fig. 28 presents a log-log plot of Maximum rate of change of heating flux versus settling time for the regulator problem. Table 18 presents the results for control action using a PI controller for the reduction in flow rate.

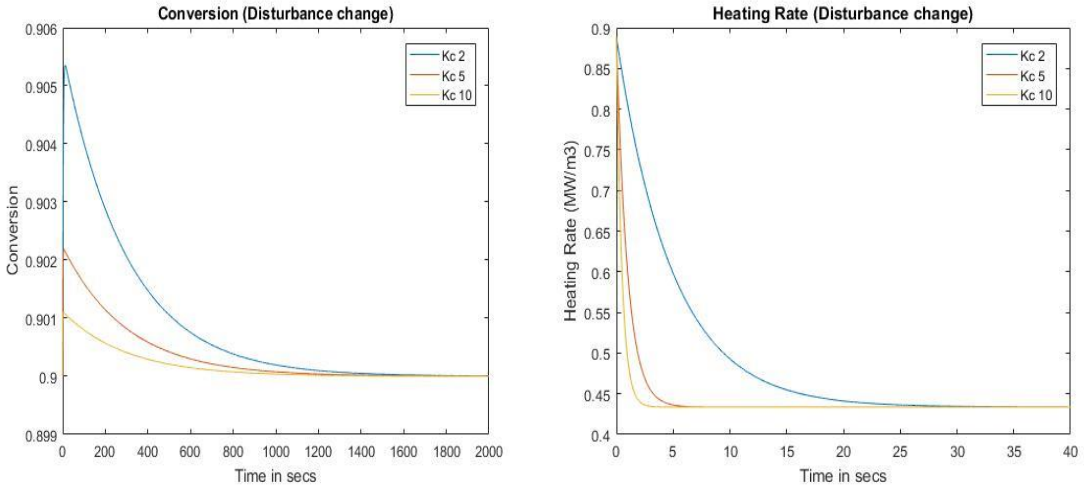

Fig 27 – Conversion and heating rate plots for different K_c values for a residence time change from 0.35 secs to 0.7 secs on conversion in a Silicon micro-channel reactor

Table 18 – **Max change in heating rate response in a Silicon micro-channel reactor**

τ_i	Kc	Settling time (s)	Maximum rate of change of heating flux (MW/m^3s)
300	1	33.42	0.1
300	2	18.68	0.2
300	5	8.36	0.4
300	10	3.74	0.9
300	25	1.68	1.9
300	50	0.71	3.3
300	100	0.23	9.2

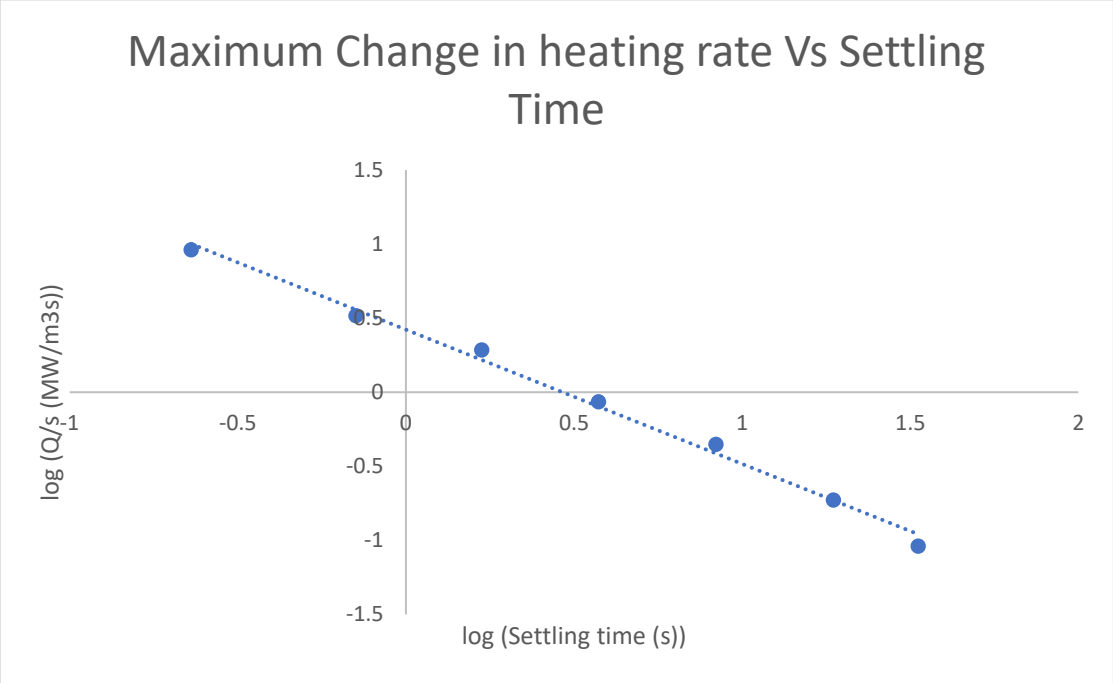

Fig. 28 - log-log plot of max change in heating rate vs settling time with a PI controller in Si

4.6) Observations from closed loop response using approximate model

1. It is possible to achieve an order of magnitude reduction in the settling time in a closed loop when compared to the open loop time constant.
2. The settling times with achievable heating rate **(35 MW/m^3) are 32.3 seconds for SS316, 23.1 seconds for Copper and 14.3 seconds for Silicon.**
3. A log-log plot for Maximum Heating Rate required versus the settling time for all the 3 materials for a set point change for conversion from 56% to 90% is shown in fig. 29.

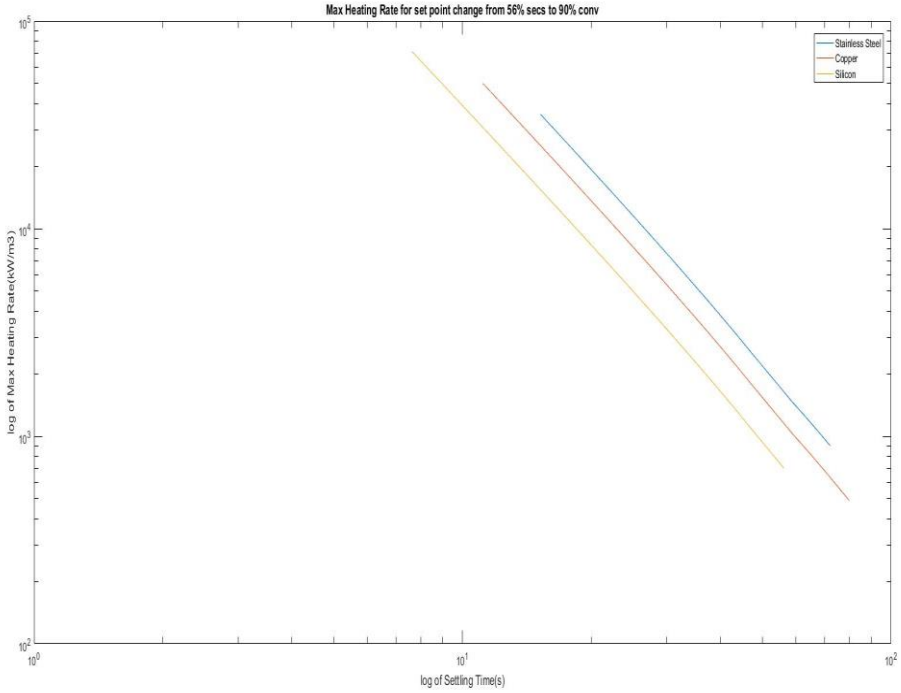

Fig. 29 – Log-log plot for material comparison for maximum heating rate vs settling time

4. A log-log plot for Maximum Change in Heating Rate required versus the settling time for all the 3 materials for a set point change for conversion from 56% to 90% is shown in fig. 30.

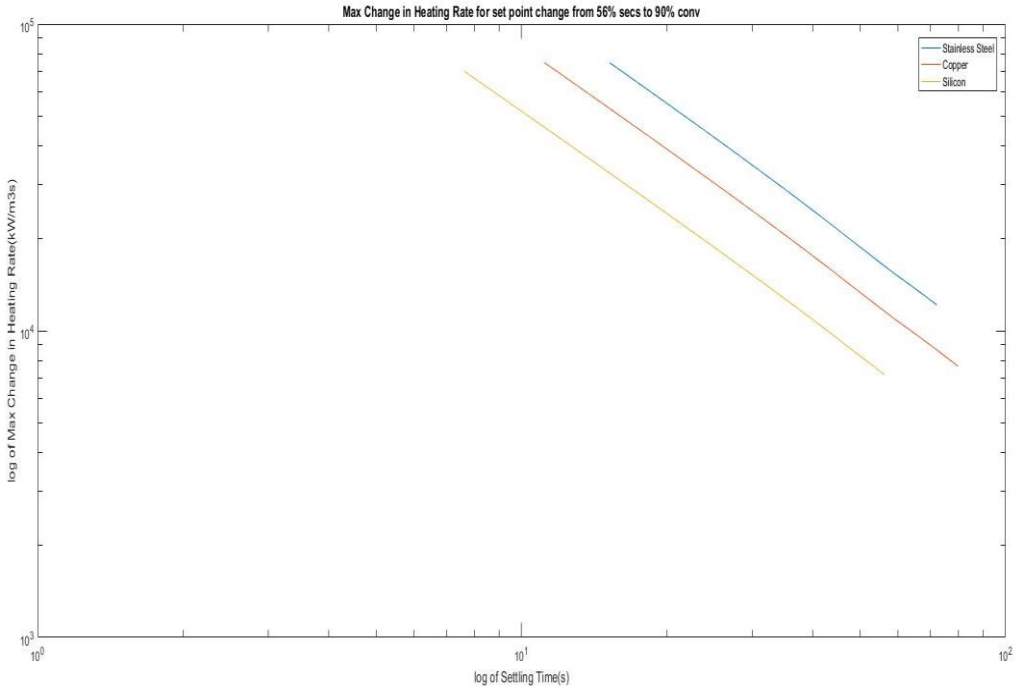

Fig. 30 – Log-log plot for material comparison for maximum change in heating rate vs settling time

In chapter 5, similar simulations were carried out for the actual PDE model and the results were compared to the state space model.

CHAPTER V

PROCESS CONTROL WITH PDE MODEL

5.1) Introduction

In this chapter, the actual PDE model developed in the chapter 2 was used in a closed loop with a PI controller and the system response characteristics were studied. The effect of material of build of micro-reactor on the control of the system was investigated. Two types of control problems were investigated for this research – Servo problem (set point change in outlet conversion) and regulator problem (Variation in the disturbance). The effect of changing the proportional gain on the settling time for the system was also investigated in detail. Section 5.2, 5.3 and 5.4 show the simulation results for servo and regulator problems for micro-channel reactors made of SS316, Copper and Silicon respectively. Section 5.5 compares the results of the state space model and the actual PDE model.

5.2) Closed loop simulations for MSR in SS316 micro-channel reactor with PDE model

5.2.1) Servo problem – Step up

Like the servo problem studied in section 4.3.1, a set point change of outlet conversion from 56% to 90% was considered. The integral time was taken as the time constant for open loop response (τ_i = 700 seconds for SS316). The proportional gain was varied and the effect on system response for outlet conversion, heating rate and change in heating rate was studied.

Fig. 31 shows the effect of proportional gain on the settling time for conversion and the heating rate.

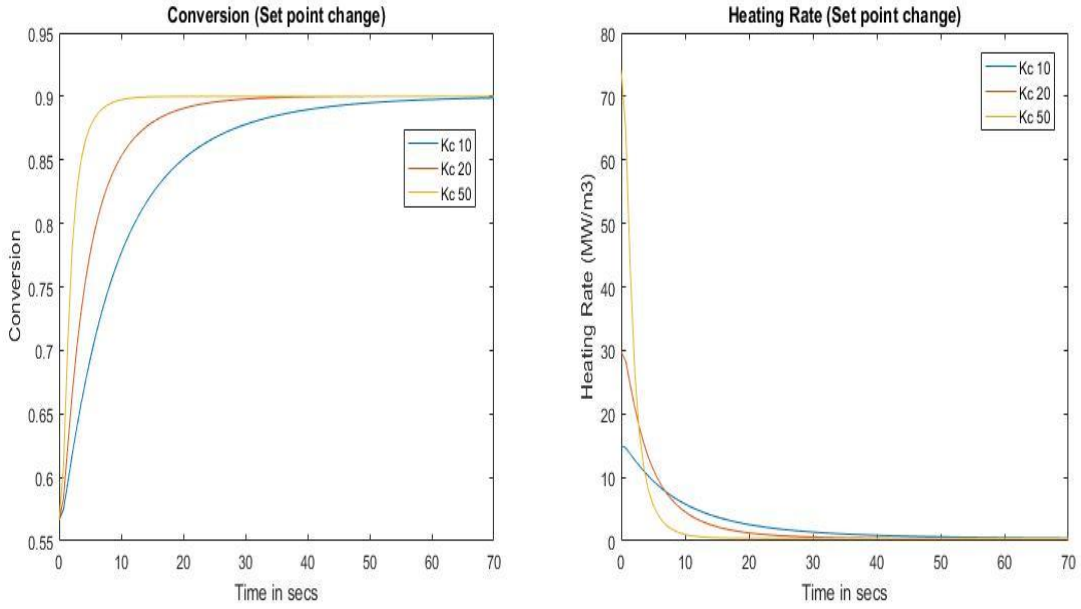

Fig. 31 – Conversion and heating rate plots for different K_c values for a set point change from 56% to 90% on conversion in a SS316 micro-channel reactor (PDE Model)

As observed from the plots, increasing the proportional gain results in faster control but also requires higher heating rates. From literature (Kawamura, Ogura, & Igarashi, 2013), a heater with maximum heat flux of 35 MW/m^3 is achievable in a micro-channel reactor.

Table 19 presents the results for control action using a PI controller. An achievable settling for a SS316 micro- channel reactor with a maximum heating rate of **35 MW/m^3 is 32.1 seconds**. As can be observed from the table 19, when K_c increases to provide very high heating rates, it leads to an overshoot in the conversion and takes more time for the system to reach a steady state of 90% outlet conversion. But considering the high heating rates are not practically possible, they can be avoided for actual design. Comparing the results for more achievable heating rates, the results obtained from PDE model and the approximate model agree with each other with less than 1% difference between the results.

Table 19 – **Heating rate response with PI controller in actual model for SS316**

τ_i	K_c	Settling Time (s)	Maximum Heating flux (MW/m^3)	Maximum rate of change of heating flux (MW/m^3s)
700	10	67.87	15	1.2
700	**25**	**31.08**	**37.3**	**7.5**
700	50	13.42	74.8	30.3
700	100	5.21	143.7	121.5
700	150	55.8	224.0	273.1
700	200	97.8	290.7	485.4
700	300	162.2	445.1	1092

5.2.2) Servo problem – Step down

Like the servo problem studied in section 4.3.2, a set point change of outlet conversion from 90% to 85% was considered. The integral time was taken as the time constant for open loop response (τ_i = 700 seconds for SS316). The proportional gain was varied and the effect on system response for outlet conversion, heating rate and change in heating rate was studied.

Fig. 30 shows the effect of proportional gain on the settling time for conversion and the heating rate.

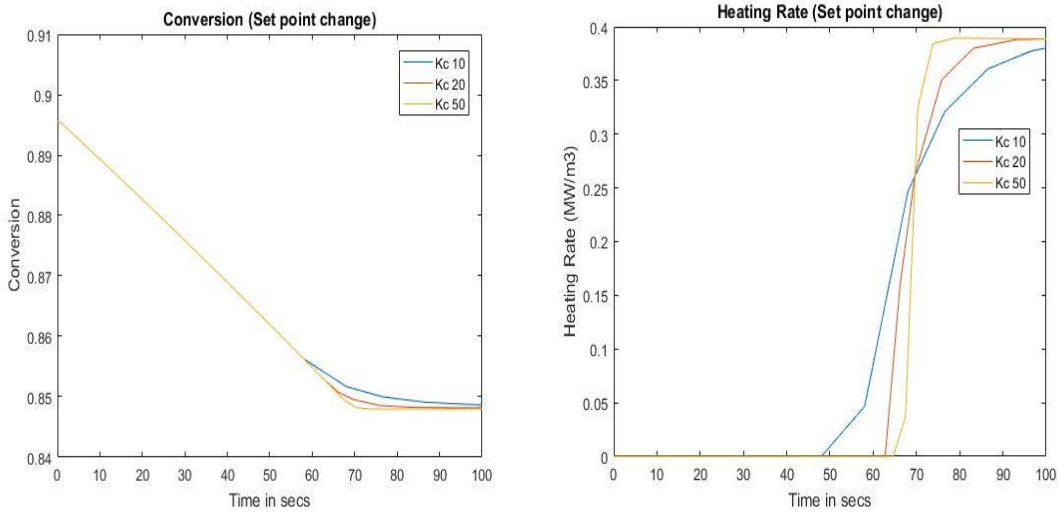

Fig. 32 – Conversion and heating rate plots for different K_c values for a set point change from 90% to 85% on conversion in a SS316 micro-channel reactor (PDE Model)

As can be observed from the heating rate plot in fig. 32, the heater shuts down at the set point step down and starts up per the value of the proportional gain. Higher the proportional gain, later the heater turns back on. Also, the conversion profiles coincide in the initial timespan for all the three different values of proportional gain which can be justified as the heater is off in that timespan in all the three cases. The settling time observed in the step-down servo problem doesn't depend strongly on the proportional gain used in the controller. The results agree with the approximate model with less than 2% difference.

5.2.3) Regulator problem

Like the regulator problem studied in section 4.3.3, a change in disturbance (residence time) from 0.35 seconds to 0.7 seconds was studied. The system was initially at an outlet conversion of 90%

and the objective was to study the response of the model to keep the system at 90% outlet conversion when the residence time was increased. The integral time was taken as the time constant for open loop response (τ_i = 700 seconds for SS316). The proportional gain was varied and the effect on system response for outlet conversion, heating rate and change in heating rate was studied.

Fig. 33 shows the effect of proportional gain on the settling time for conversion and the heating rate. For the regulator problem for step up in residence time, the maximum heating rate is not a constraint. Only important parameter here was to consider that the heater didn't start acting like a cooler for faster control.

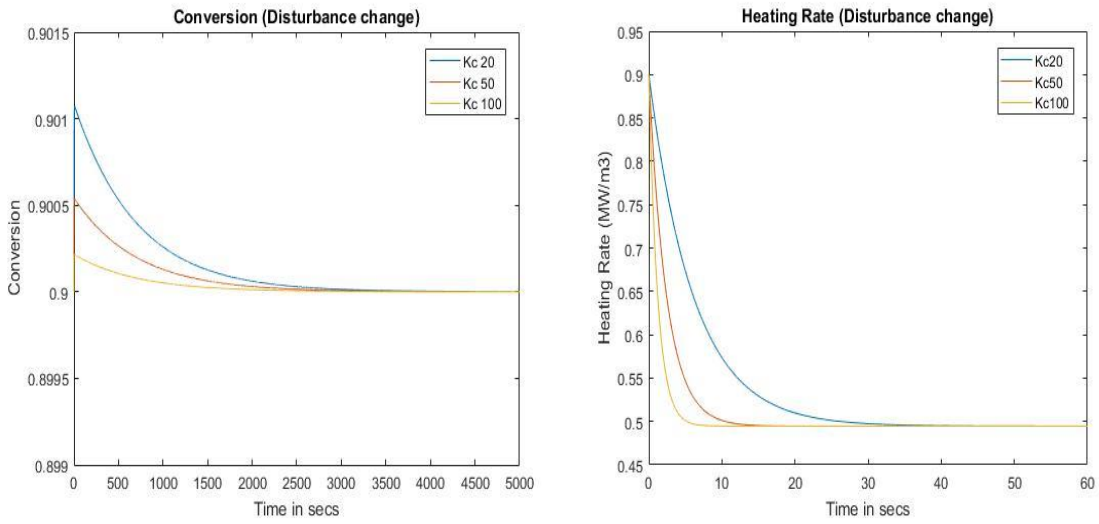

Fig 33 – Conversion and heating rate plots for different K_c values for a residence time change from 0.35 secs to 0.7 secs on conversion in a SS316 micro-channel reactor (PDE Model)

As can be observed from the heating rate plot in fig. 33, maximum heating rate is always the highest at initial time of the step change, hence the only criteria to define the effectiveness of the control is the speed of response of the heater, faster the change in heating rate, faster will be the

control for the system. Table 20 presents the results for control action using a PI controller for the reduction in flow rate.

Table 20 – **Max change in heating rate response in actual model for SS316**

τ_i	**Kc**	**Settling time (s)**	**Maximum rate of change of heating flux (MW/m^3s)**
700	10	45.8	0.034
700	25	26.72	0.082
700	50	15.7	0.162
700	100	7.11	0.37
700	150	6.5	0.493
700	200	3.86	0.61
700	300	2.4	0.876

Comparing the results for more achievable heating rates, the results obtained from PDE model and the approximate model agree with each other with less than 1% difference between the results.

5.3) Closed loop simulations for MSR in Copper micro-channel reactor with state space model

5.3.1) Servo problem

Like the case of stainless steel 316, the servo problem for micro-channel reactor made of Copper investigated the effect of a PI controller for control of the state-space model when a set point change was made from 56% to 90% on the outlet conversion of methanol. The integral time was taken as the time constant for open loop response (τ_i = 500 seconds for Copper). The proportional

gain was varied and the effect on system response for outlet conversion, heating rate and change in heating rate was studied.

Fig. 34 shows the effect of proportional gain on the settling time for conversion and the heating rate.

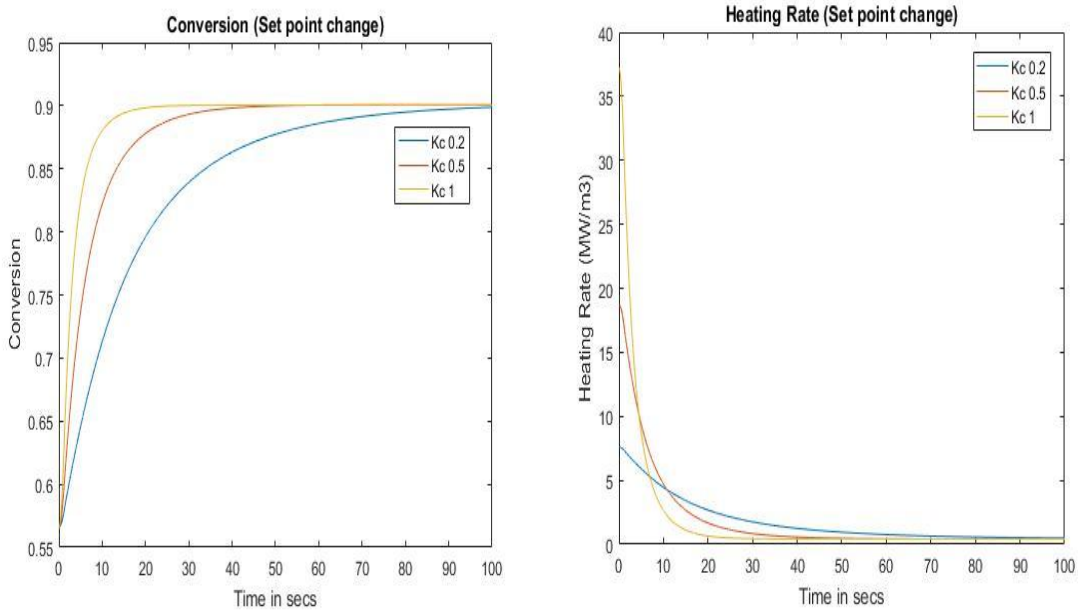

Fig. 34 – Conversion and heating rate plots for different K_c values for a set point change from 56% to 90% on conversion in a Copper micro-channel reactor (PDE Model)

Like in section 5.2.1; increasing the proportional gain results in faster control but also requires higher heating rates.

Table 21 presents the results for control action using a PI controller. An achievable settling time for a copper micro- channel reactor with a maximum heating rate of **35 MW/m^3 is 23.3 seconds**.

Table 21 – **Heating rate response with PI controller in actual model for Cu**

τ_i	K_c	Settling Time (s)	Maximum Heating flux (MW/m^3)	Maximum rate of change of heating flux (MW/m^3s)
500	0.1	196.4	0.398	0.1
500	0.5	46.2	20.32	3.08
500	1	22.3	37.52	12.4
500	2	11.91	74.9	50
500	5	7.81	185.2	310.1
500	10	2.96	367.2	1196
500	25	1.33	942.8	7205
500	50	1.12	1885.4	29827

5.3.2) Regulator problem

Like in section 5.2.3, the regulator problem studied for this research was with a change in disturbance (residence time) from 0.35 seconds to 0.7 seconds. The integral time was taken as the time constant for open loop response (τ_i = 500 seconds for Copper). The proportional gain was varied and the effect on system response for outlet conversion, heating rate and change in heating rate was studied.

Fig. 35 shows the effect of proportional gain on the settling time for conversion and the heating rate.

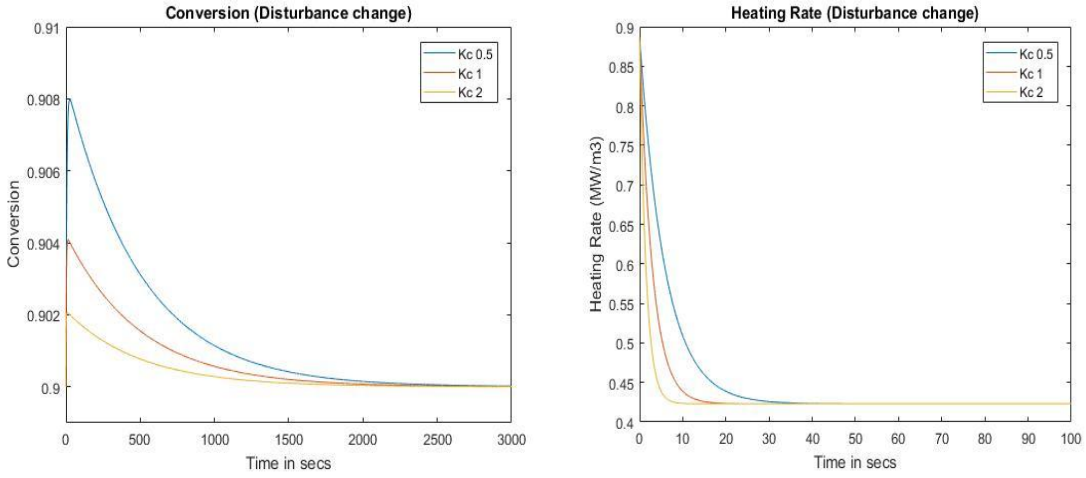

Fig 35 – Conversion and heating rate plots for different K_c values for a residence time change from 0.35 secs to 0.7 secs on conversion in a Copper micro-channel reactor (PDE Model)

As can be observed from the heating rate plot in fig. 35, maximum heating rate is always the highest at initial time of the step change, hence the only criteria to define the effectiveness of the control is the speed of response of the heater, faster the change in heating rate, faster will be the control for the system. Table 22 presents the results for control action using a PI controller for the reduction in flow rate.

Table 22 – **Max change in heating rate response in actual model for Cu**

τ_i	Kc	Settling time (s)	Maximum rate of change of heating flux (MW/m^3s)
500	1	7.68	0.19
500	2	5.21	0.288
500	5	2.43	0.71
500	10	1.29	1.38
500	25	0.71	2.74
500	50	0.84	4.5

5.4) Closed loop simulations for MSR in Silicon micro-channel reactor with state space model

5.4.1) Servo problem

Like the case of stainless steel 316 and copper in sections 5.2.1 and 5.3.1 respectively, the servo problem for micro-channel reactor made of Silicon investigated the effect of a PI controller for control of the state-space model when a set point change was made from 56% to 90% on the outlet conversion of methanol. The integral time was taken as the time constant for open loop response (τ_i = 300 seconds for Silicon). The proportional gain was varied and the effect on system response for outlet conversion, heating rate and change in heating rate was studied.

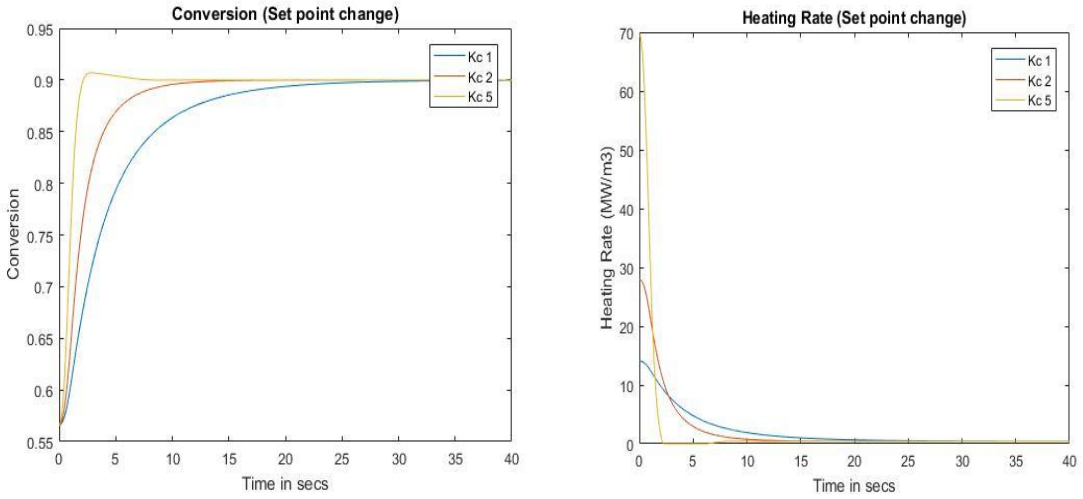

Fig. 36 – Conversion and heating rate plots for different K_c values for a set point change from 56% to 90% on conversion in a Silicon micro-channel reactor (PDE Model)

Table 23 – **Heating rate response with PI controller in actual model for Si**

τ_i	K_c	Settling Time (s)	Maximum Heating flux (MW/m^3)	Maximum rate of change of heating flux (MW/m^3s)
300	1	31.23	14.85	0.07
300	2	17.18	28.41	0.28
300	5	9.21	69.2	1.65
300	10	5.21	136.4	6.72
300	25	2.65	274.1	38.94
300	50	1.54	673.8	161.2
300	100	1.63	1371.6	631.54
300	150	1.42	1995.6	1387.93

Like in section 5.2.1 and 5.3.1; increasing the proportional gain results in faster control but also requires higher heating rates. Table 23 presents the results for control action using a PI controller. An achievable settling time for a copper micro- channel reactor with a maximum heating rate of **35 MW/m^3 is 14.3 seconds**. Fig. 36 shows the effect of proportional gain on the settling time for conversion and the heating rate.

5.4.2) Regulator problem

Like in section 5.2.3 and 5.3.2 for SS316 and Copper, the regulator problem studied for this research was with a change in disturbance (residence time) from 0.35 seconds to 0.7 seconds. The integral time was taken as the time constant for open loop response (τ_i = 300 seconds for Silicon). The proportional gain was varied and the effect on system response for outlet conversion, heating rate and change in heating rate was studied.

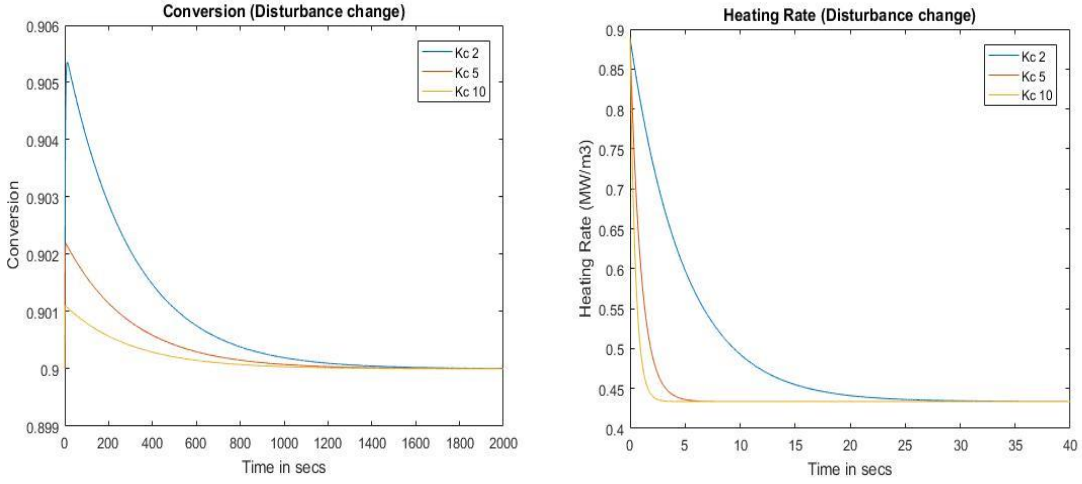

Fig 37 – Conversion and heating rate plots for different K_c values for a residence time change from 0.35 secs to 0.7 secs on conversion in a Silicon micro-channel reactor (PDE Model)

Fig. 37 shows the effect of proportional gain on the settling time for conversion and the heating rate. As can be observed from the heating rate plot in fig. 37, maximum heating rate is always the highest at initial time of the step change, hence the only criteria to define the effectiveness of the control is the speed of response of the heater, faster the change in heating rate, faster will be the control for the system.

As can be observed from the heating rate plot in fig. 37, maximum heating rate is always the highest at initial time of the step change, hence the only criteria to define the effectiveness of the control is the speed of response of the heater, faster the change in heating rate, faster will be the control for the system. Table 24 presents the results for control action using a PI controller for the reduction in flow rate.

Table 24 – **Max change in heating rate response in actual model for Si**

τ_i	**Kc**	**Settling time (s)**	**Maximum rate of change of heating flux (MW/m^3s)**
300	1	34.1	0.098
300	2	19.23	0.193
300	5	8.39	0.4
300	10	3.81	0.89
300	25	1.73	1.86
300	50	1.33	2.89
300	100	1.45	7.36

5.5) Comparison of control results between state space model and PDE model

1. The PDE model and state space model give comparable response with an error of less than 2% for both the servo and the regulator problem and hence the state space model can be considered a good approximation of the PDE model for actual controller design.
2. Settling times in the range of 20 seconds to 50 seconds are possible for all the three materials considered here for the heaters currently available in the market for micro-reactors.
3. Fig. 38 represents a comparative plot of the response of outlet conversion of methanol in a SS316 micro-channel reactor with a proportional gain for 10 and 100 for a set point change from 56% to 90% on using the PDE model and the state space (approximate) model.

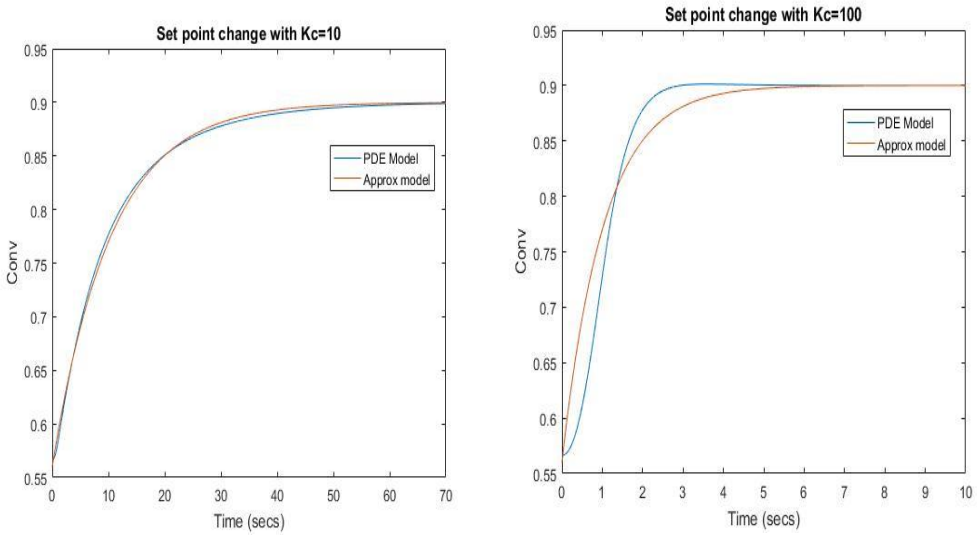

Fig. 38 – Comparison of PDE Model and Approximate model with different proportional gains

4. The response is nearly identical at low proportional gains and varies a bit as proportional gain increases.

CHAPTER VI
CONCLUSION AND FUTURE WORK

6.1) Conclusion

The 1-D open loop model used for this research shows close agreement with the conversion and temperature profiles achieved experimentally by (Kundu, 2006). The open loop and closed loop simulations displayed the dependence of the settling time on the material of construction of the micro-reactor by a factor of the thermal capacity of the wall. In terms of dimensionless groups, this can be represented as a ratio of Fo number to CP. Silicon having the lowest ratio of Fo number to CP shows the fastest settling times. The open loop step changes displayed first order characteristics with non-linearity which prompted the use of PI controller with Hammerstein model for controls studies. Settling times in the range of 10 seconds to 50 seconds are possible for all the three materials considered here for the heaters currently available in the market for micro-reactors in closed loop. For the step-up case in the servo problems, the maximum heat flux that can be provided by an external heater is the constraint to how fast the system can reach the desired steady state. For the step-down regulator problem, the constraint is found to be the maximum change in heat flux that is achievable. The closed loop dynamic responses by using the state space model and PDE model closely agree with each other. For lower values of controller gains (Kc <=10 in SS316 micro reactor), both models are identical within 1%. For higher values of controller gains (Kc >=50 in SS316 micro reactor), the models show differences of around 5%.

6.2) Future works

1. There is substantial scope for incorporating a block of micro-channel reactor inside a car engine and incorporating it with a fuel cell so to provide hydrogen directly to the fuel cell from the MSR reaction in the micro-reactor. The control of the MSR reaction in the micro-channel reactor will be of great importance in such an application.

2. There is scope for replacing the heating plate and substituting it with another micro-channel in which an exothermic reaction (for ex. Methane combustion) takes place so to provide the required heat for the MSR reaction. Studying the effects on control for co-current and counter current flow for such a system will be an interesting study and can find practical uses in natural gas wells.

REFERENCES

Amar Equipments. (2016). Retrieved from Amar Equipments Website.

Anandanatarajan, R. (2005). Limitations of a PI Controller for a first order nonlinear process with dead time. *ISA Transactions*, 185-199.

Astrom, K. J. (2002). *Control System Design.* New York: Springer.

Behrens, M., & Armbruster, M. (2012). Methanol steam reforming. *Catalysis for Alternate Energy Generation*, 175-235.

Breen, R. B. (2002). Metal -catalysed steam reforming of ethanol in the production of hydrogen for fuel cell applications. *Applied Catalysis*, 65-74.

Brown, L. (2001). A comparative study of fuels for onboard hydrogen production for fuel cell powered automobiles. *International Journal for Hydrogen Power*, 381-397.

Cao, G. X. (2003). Kinetics studies of methanol steam reforming over Pd/ZnO catalyst using a microchannel reactor. *Applied Catalysis*, 19-29.

Chalk, J. F. (2006). Key challenges and recent progress in batteries, fuel cells, and hydrogen storage for clean energy systems. *Journal of power sources*, 73-80.

Cverna, F. (2002). *Thermal Properties of Metals.* ASM Ready Reference.

Dinca, P. G. (2008). Design of a PID controller for a PCR Microreactor. *IEEE Transactions on Education*, 116-125.

Distefano, J., Stubberud, A., & Williams, I. (1967). *Feedback and Control Systems, 2nd Edition.* McGraw-Hill.

Dyer, C. K. (2002). Fuel Cells for portable power. *Fuel Cells Bulletin*, 8-9.

Echave, O. S. (2013). Effect of alloy on micro-structured reactors for methanol steam reforming. *Catalysis Today*, 145-154.

Ehrfeld, V. H. (2002). *Ullmann's Encyclopedia of Industrail Chemistry.* Wiley.

Frank P., I. D. (2011). *Fundamentals of Heat and Mass Transfer, 7th Edition.* Wiley.

Froment, K. B. (1990). *Chemical Reaction Analysis and Design, Second Edition.* John Wiley & Sons.

Grewal, B. (2008). *Higher Engineering Mathematics, 42nd Edition.* Khanna Publishers.

Grossman, H.-G. R. (2007). *Numerical Treatment of Partial Differential Equations.* Springer Science and Business.

Hangos, K., & R. Lakner, M. G. (2001). *Intelligent control Systems: An introduction with Examples.* Springer.

Higham, N. (2002). *Accuracy and Stability of Numerical Algorithms, 2nd Edition.* SIAM.

Hinrichsen D, P. A. (2005). *Mathematical systems theory I: Modelling, State space analysis, stability and robustness.* Springer.

Karim, T. C. (2008). Controlling ZnO morphology for improved methanol steam reforming activity. *Physical Chemistry Chemical Physics*, 5584-5590.

Kawamura, Y., Ogura, N., & Igarashi, A. (2013). Hydrogen Production by Methanol Steam Reforming using Microreactor. *Journal of Japan Petroleum Institute,* 288-297.

Kendall, D. (2006). *Chemical Reactors: Basic Control Strategies.* Springer.

Kolb, V. H. (2005). *Reaction Engineering.* Chemical Engineering Journal.

Kundu, J. P. (2006). Micro-channel reactor for steam reforming of methanol. *Fuel*, 1331-1336.

Levenspiel, O. (1962). *Chemical Reaction Engineering.* Springer.

Moreno, B. A. (2008). Parametric study of Solid -Phase Axial heat conduction in thermally integrated Microchannel Networks. *Industrial & Engineering Chemistry Research*, 9040-9054.

Nelles, O. (2001). *Nonlinear System Identification.* Sringer.

Ogata, K. (1997). *Modern Control Engineering, 3rd Edition.* New Jersey: Prentice-Hall.

Ogunnaike, W. H. (1994). *Process Dynamics, Modeling and Control.* New York: Oxford University Press.

Olah, G. A. (2006). *Beyond Oila nd Gas: The Methanol Economy.* Wiley.

Olver, P. (2013). *Introduction to Partial Differential Equations.* Springer Science and Business Media.

Palo, R. A. (2007). Methanol steam reforming for hydrogen production. *American Chemical Society*, pp. 3992-4021.

Pan, Z. F. (2015). Reaction characteristics of methanol steam reforming inside mesh microchannel reactor. *Internation Journal for Hydrogen Power*, 1441-1452.

Peppley, J. C. (1999). Methanol steam reforming on Cu/ZnO/Al2O3. *Catalysis*, 21-29.

Powell, D. (2004). *Advanced System Dynamics and Control.* Dept. of Mechanical Engineering, Massachusetts Institute of Technology.

Serra, D. P. (2013). *Encyclopedia Of Polymer Science and Technology, Edition: 4.* Wiley.

Smith, A. (2003). Estimating a state-space model from point process observations. *Neural Computation*, 965-991.

Smith, A., & L., C. (2009). *Practical Process Control Tuning and Troubleshooting.* Wiley.

Suwa, S.-i. I. (2004). Comparative study between Zn-Pd/C and Pd/ZnO catalysts for steam reforming of methanol. *Applied Catalysis*, 9-16.

Swaney, R., & Rawlings, J. (2014). *Estimation of Parameters from Data.* Department of Chemical & Biological Engineering, University of Wisconsin-Madison.

Takahashi, N. T. (1982). The mechanism of steam reforming of methanol over a copper-silica catalyst. *Applied catalysis*, 363-366.

TeGrotenhuis, W. (2008). Novel microreactor design for balancing heat and mass transfer. *Catalysis*, 122-134.

Tronconi, I. N. (2005). Modelling of a SCR catalytic converter for diesel exhaust after treatment: Dynamic effects at low temperature. *Catalysis Today*, 529-536.

Ueberhuber, C. W. (1997). *Numerical Computation 1: Methods, Software and Analysis.* Springer.

Vazquez, P. S. (2015). Reactor design and catalylsts testing for hydrogen production by methanol steam reforming for fuel cell applications. *International journal for Hydrogen power*, 924-935.

Verhaegen, M. (1994). Identification of the deterministic part of MIMO state space models given in innovations form from input-output data. *Automatica*, 61-74.

Verwijs, P. K. (1995). Reactor operating procedures for startup of continuously operated chemical plants. *Reactors, Kinetics and Catalysis*, 148-158.

Wills, T. B. (2012). Identifiacation of Hammerstein-Wiener Models. *Automatica*, 67-72.

APPENDIX A :

MATLAB CODES

Open loop model -

```
function [] = openloop()
N=300; % 3*(# of spatial discretizations)
x=linspace(0,1,N/3); % Discretizing the spatial axis for plotting
uinitial=zeros(N,1); % Initialing the Initial condition vector
tspan = [0 7000];
% Initial condition for dimensionless concentration for the reaction
stream
for i=1:N/3
uinitial(i)= 1; %was 1
end
% Initial condition for dimensionless temp for the reaction stream
for i=N/3+1:2*N/3
uinitial(i)=0;
end
% Initial condition for dimensionless temperature for the wall
for i=(2*N)/3+1:N
uinitial(i)=0;
end

uinitial = uinitial';
% Using ode solver to solve the system of discretized pde
[T,Y] = ode23s(@sub,tspan,uinitial);
[a, b]=size(Y);

% Converting the output matrix from ode solver to give us only
dimensionless concentration with time and spatially
u=zeros(a,N/3);
for i=1:a
    for j = 1:(b/3)
        u(i,j)= Y(i,j);
    end
end

save('heatingcoilconcinitial.mat','u') % Saving the matrix for IC of
bvp4c code

% Converting the output matrix from ode solver to give us only
dimensionless temperature with time and spatially
v=zeros(a,N/3);
for i=1:a
    for j = (b/3+1):(2*b)/3
        v(i,j-b/3)= Y(i,j);
    end
end
```

```
save('heatingcoiltempinitial.mat','v') % Saving the matrix for IC of
bvp4c code

% Converting the output matrix from ode solver to give us only
dimensionless temperature for the wall with time and spatially
vw=zeros(a,N/3);
for i=1:a
    for j = ((2*b)/3+1):b
        vw(i,j-(2*b)/3)= Y(i,j);
    end
end
save('heatingcoiltempwinitial.mat','vw') % Saving the matrix for IC
bvp4c code

plot(T,1-u(:,N/3))
Outlet_stream_conv = 1-u(a,:);
Outlet_stream_temp = v(a,N/3);
Inlet_wall_temp = vw(a,2);
end

function dudt=sub(~,u)
N=300; % Definning the number of points in spatial axis
x=linspace(0,3,N); % Discretizing the spatial axis
deltax=x(2)-x(1); % Definning each interval size
dudt = zeros(N,1); % Initializing the vector for all 3 PDEs combined

% The boundary conditions are--
u(1)=1; u(N/3+1)= 0; % Inlet conditions for concentration and
temperature

u((2*N)/3+1)= u((2*N)/3+2); u(N)=u(N-1); % Adiabatic boundary
conditions for the wall

% The dimensionless groups are--
Da = 20.6; alpha= 20.25; gamma= -0.636 ;NTU=188; CP=11.7; theta=0.25;
Fo=0.00293; psi=-0.045;

% Order of the reactions
n=1;

for i=2:N/3
    % Dimensionless concentration for the reaction stream
    dudt(i) = -(u(i)-u(i-1))/deltax -
Da*theta*exp((alpha*gamma*u(N/3+i-1))/(1+gamma*u(N/3+i-1)))*u(i-1)^n;
    % Dimensionless temp for the reaction stream

    dudt(N/3+i) = -(u(N/3+i)-u(N/3+i-1))/deltax +
Da*theta*exp((alpha*gamma*u(N/3+i-1))/(1+gamma*u(N/3+i-1)))*u(i-1)^n -
NTU*theta*(u(N/3+i-1)-u((2*N)/3+i-1));
end

for i=2:N/3-1
```

```
    % Dimensionless temperature for the wall
    dudt((2*N)/3+i) = Fo*theta*((u((2*N)/3+i+1)+u((2*N)/3+i-1)-
2*u((2*N)/3+i))/deltax^2) + Fo*theta*(NTU/CP*(u(N/3+i-1)-u((2*N)/3+i-
1))+psi);
end
end
```

Closed loop model with approximate function –

```
function [] = project()
% N=50;
% n=1000*N;
tspan = linspace(0,70,6000);
yinitial = [0.56 0]; %Initital conversion and error
taui=700; Kc=10;Xss=0.90;psib = -0.0445;
[T,Y] = ode23s(@derivative,tspan,yinitial);   % Using ode solver
Ep = Xss-Y(:,1);
psi=psib-Kc*(Ep+Y(:,2)/taui);
Psi = 16*563.15*(-0.673)*psi/(0.037^2*1000);
A=Y(:,1);
slope=diff(psi)./diff(T);
% convslope=diff(A)./diff(T);
X=[slope T(2:end)];
for i=1:length(slope)
    if abs(slope(i))<0.1 && abs(slope(i))>0.001
        Time=T(i+1);
    end
end
x= Y(:,1);
t=T;
figure
plot(t,x)
save ('convapp.mat','x')
save ('timeapp.mat','t')
save ('psiapp.mat','Psi')

% [max_slope, idx] = max(slope);
% [min_slope,idy] = min(slope);
% A=T(idx);
% B=T(idy);
% Max_heating_rate=[max_slope A]
% Min_heating_rate=[min_slope B]
% [max_Heating, ida] = max(abs(psi));
% [min_Heating, idb]= min(abs(psi));
% C=T(ida);
% D=T(idb);
% Min_heating=[max_Heating C]
% Max_heating=[min_Heating D]
%
% Max_heating=max(abs(psi));
% Min_heating=min(abs(psi));
```

```
% yyaxis left
% plot(T,Y(:,1)) % Plotting change in conversion
% ylabel('Conversion')
% ylim([0 1])
% hold on
% yyaxis right
% plot(T,psi,'*') % Plotting change in heating rate
% ylabel('Heating rate')
% xlabel('time in secs.')
% title ('Conversion vs time')
% legend ('Conversion','Heating Rate')

A=Y(:,1);
P1=psi;
T1=T;
save('kc20.mat','A')
save('kc20t.mat','T1')
save('kc20p.mat','P1')

% B=Y(:,1);
% P2=psi;
% T2=T;
% save('kc50.mat','B')
% save('kc50t.mat','T2')
% save('kc50p.mat','P2')

% C=Y(:,1);
% P3=psi;
% T3=T;
% save('kc100.mat','C')
% save('kc100t.mat','T3')
% save('kc100p.mat','P3')

end

 function dy = derivative(~,y)
dy = zeros(2,1);

% SS316
tau=700; A = 0.116; B = -0.196; C = -9.32;D = 0.18;
taui=700; Kc=10;psib = -0.0445;

% % Copper
% tau=500; A = 0.1234; B = -7.81; C = -230.9; D = 0.17;
% taui=500; Kc=2;psib =-0.008;

% % Silicon
% tau=300; A = 0.1177; B = -2.413; C = -85.2; D = 0.18;
% taui=300; Kc=2;psib =-0.0214;

Xss=0.90;Ep = Xss-y(1);theta = 0.7;
```

```
psi=psib-Kc*(Ep+y(2)/taui);

% Closed loop control
dy(1) = (A*theta+B*psi+C*psi*theta+D)/tau-y(1)/tau;
% Integral Error
dy(2) = Xss-y(1);
 end
```

Closed loop with PDE model –

```
function [] = kunduPDE()
N=300; % Number of points in the time step
tspan = [0 700]; % Definning the time interval of study
x=linspace(0,1,N/3); % Discretizing the spatial axis for plotting
uinitial=zeros(N+1,1); % Initialing the Initial condition vector

load heatingcoilconcinitial.mat;
load heatingcoiltempinitial.mat;
load heatingcoiltempwinitial.mat;

% Definning the initial conditions as the steady state solutions from
PDE code
for i = 1:length(x)
    uinitial(i)=u(end,i);
    uinitial(N/3+i)=v(end,i);
    uinitial((2*N)/3+i)=vw(end,i);
end

uinitial (N+1) = 0;

uinitial = uinitial';
% Using ode solver to solve the system of discretized pde
[T,Y] = ode23s(@sub,tspan,uinitial);
[a, b]=size(Y);

u=zeros(a,N/3);
for i=1:a
    for j = 1:(b/3)
        u(i,j)= Y(i,j);
    end
end

v=zeros(a,N/3-1);
for i=1:a
    for j = 102:200
        v(i,j-101)= Y(i,j);
    end
end
ts= v*(205-563)+563;
```

```
Ts= max(ts);
TempStream = max(Ts)

vw=zeros(a,N/3-2);
for i=1:a
    for j = 202:299
        vw(i,j-201)= Y(i,j);
    end
end
tw=vw*(205-563)+563;
Tw=max(tw);
TempWall = max(Tw)
%
X=1-u(:,N/3);
z=Y(:,N+1);
convslope=diff(X)./diff(T);
for i=1:length(convslope)
    if abs(convslope(i))<0.1 && abs(convslope(i))>0.0001
        Time=T(i+1);
    end
end
ResTime = Time
% figure
% plot(T,X)
%
taui=1500; Kc=1; Xss=0.9; psib = -0.0445;
Ep = (Xss-X);
psi=psib-Kc*(Ep+z/taui);
PSI = 16*563.15*(-0.673)*psi/(0.037^2*1000);
MaxPsi = max(PSI)
slope=diff(PSI)./diff(T);
MaxHeatingRateChnage = max(abs(slope))
% figure
% plot (T,PSI)
% save ('convpde.mat','X')
% save ('timepde.mat','T')
% save ('psipde.mat','PSI')
end

function dudt=sub(~,u)
N=300; % Definning the number of points in spatial axis
x=linspace(0,3,N); % Discretizing the spatial axis
deltax=x(2)-x(1); % Definning each interval size
dudt = zeros(N+1,1); % Initializing the vector for all 5 PDEs combined

% The boundary conditions are--
u(1)=1; u(N/3+1)= 0; % Inlet conditions for concentration and
temperature

u((2*N)/3+1)= u((2*N)/3+2); u(N)=u(N-1); % Adiabatic boundary
conditions for the wall

% The dimensionless groups are-
```

```
Da = 20.6; alpha= 20.25; gamma= -0.636 ;NTU=188; CP=11.7; theta=0.7;
Fo=0.0029;
%psi=-0.095;

% Control trial
taui=1500; Kc=1;Xss=0.9;psib = -0.0445; Ep =Xss-(1-u(N/3));
psi=psib-Kc*(Ep+u(N+1)/taui);

% Order of the reactions
n=1;

for i=2:N/3
    % Dimensionless concentration for the first stream
    dudt(i) = -(u(i)-u(i-1))/deltax -
Da*theta*exp((alpha*gamma*u(N/3+i-1))/(1+gamma*u(N/3+i-1)))*u(i-1)^n;
    % Dimensionless concentration for the second stream
    dudt(N/3+i) = -(u(N/3+i)-u(N/3+i-1))/deltax +
Da*theta*exp((alpha*gamma*u(N/3+i-1))/(1+gamma*u(N/3+i-1)))*u(i-1)^n -
NTU*theta*(u(N/3+i-1)-u((2*N)/3+i-1));
end

for i=2:N/3-1
    % Dimensionless temperature for the wall
    dudt((2*N)/3+i) = Fo*theta*((u((2*N)/3+i+1)+u((2*N)/3+i-1)-
2*u((2*N)/3+i))/deltax^2) + Fo*theta*(NTU/CP*(u(N/3+i-1)-u((2*N)/3+i-
1))+psi);
end
% Error for PI controller

dudt(N+1)= Xss - (1-u(N/3));
end
```